SOUTHERN CALIFORNIA PARTICLE SUPERSITE

Progress Report for Period September 1, 2002 – December 31, 2002

United States Environmental Protection Agency

Principal Investigators: John R. Froines, Ph.D., UCLA School of Public Health

Constantinos Sioutas, Sc.D., USC School of Engineering

1. Introduction

The overall objective of the Southern California Particle Supersite is to conduct research and monitoring that contributes to a better understanding of the measurement, sources, size distribution, chemical composition and physical state, spatial and temporal variability, and health effects of suspended particulate matter (PM) in the Los Angeles Basin (LAB). This report addresses the period from September 1, 2002 through December 1, 2002. It is divided into 13 sections, each addressing a specific research area. Furthermore, a major portion of the information included in this report has been either submitted or accepted for publication in peer-reviewed journals. Below is a list of manuscripts either submitted or accepted for publication which were produced to-date through the Southern California Supersite funds and in which the EPA Supersite program has been acknowledged.

2. Publications

1. Singh, M., Jaques, P. and Sioutas, C. "Particle-bound metals in source and receptor sites of the Los Angeles Basin". *Atmospheric Environment,* 36(10): 1675-168, 2002 .

2. Kim, S., Shi, S., Zhu, Y., Hinds, W.C., and Sioutas, C. "Size Distribution, Diurnal and Seasonal Trends of Ultrafine Particles in Source and Receptor Sites of the Los Angeles Basin". *Journal of Air and Waste Management Association*, 52:174-185, 2002

3. Li, N., Kim, S., Wang, M., Froines, J.R., Sioutas, C. and Nel, A. "Use of a Stratified Oxidative Stress Model to Study the Biological Effects of Ambient Concentrated and Diesel Exhaust Particulate Matter". *Inhalation Toxicology*, 14(5): 459-486, 2002

4. Zhu, Y., Hinds, W.C., Kim, S., Shen, S. and Sioutas, C. "Study on Ultrafine Particles and other Vehicular Pollutants near a Busy Highway Dominated by Diesel Traffic". *Atmospheric Environment*. 36, 4375-4383, 2002

5. Eiguren-Fernandez A., Miguel A.H, Jaques, P. and Sioutas, C. "Evaluation of a Denuder-MOUDI-PUF Sampling System to Determine the Size Distribution of Semivolatile Polycyclic Aromatic Hydrocarbons in the Atmosphere". *Aerosol Science and* Technology, 37: 201-209, 2003

6. Zhu, Y., Hinds, W.C., Kim, S and Sioutas, C. "Concentration and Size Distribution of Ultrafine Particles near a Major Highway". *Journal of Air and Waste Management Association*, 52:1032-1042, 2002

7. Geller, M.D., Kim, S. Misra, C., Sioutas, C., Olson, B.A and Marple, V.A. "Methodology for measuring size-dependent chemical composition of ultrafine particles " *Aerosol Science and Technology*, 36(6): 748-763, 2002

8. Misra, C., Kim S., Shen S. and Sioutas C. "Design and evaluation of a high-flow rate, very low pressure drop impactor for separation and collection of fine from ultrafine particles". *Journal of Aerosol Science*, 33(5): 735-752, 2002

9. Fine, P.M., Hering, S.V., Jaques P.A. and Sioutas, C. "Performance Evaluation and Field Use of a Continuous Monitor for Measuring Size-Segregated PM2.5 Particulate Nitrate". *Aerosol Science and Technology*, 37: 342-354, 2003

10. Misra, C., Geller, M.D., Solomon, P.A. and Sioutas, C. "Development of a PM10 Inertial Impactor for Coarse Particle Measurement and Speciation." *Aerosol Science and Technology,* 37:271-282, 2003

11. Stolzenburg, M.R., Dutcher, D., Kirby, B., Kreisberg, N. and Hering, S.V. (2002). Automated Measurement of the Size Distribution of Airborne Particulate Nitrate. Submitted to *Aerosol Science & Technology*, April 002

12. Shen, S., Zhu, Y., Jaques PA and Sioutas C. "Evaluation of the SMPS-APS system as a Continuous Monitor for PM2.5 and PM10". *Atmospheric Environment*, 36, 3939-3950, 2002

13. Emma Di Stefano Yoshito Kumagai, Antonio H. Miguel, Arantzazu Eiguren, Takahiro Kobayashi, Ed Avol and John R. Froines "Determination of four Quinones/Hydroquinones in Diesel Exhaust Particles and Atmospheric PM2.5" Submitted to *Aerosol Science and Technology*, October 2002

14. Philip M. Fine, Si Shen, Michael Geller and Constantinos Sioutas "Inferring the sources of PM2.5 at downwind receptor sites in the Los Angeles Basin using multiple semi-continuous monitors "Submitted to *Aerosol Science and Technology*, October 2002

15. Jeff Ambs, Peter Jaques and Constantinos Sioutas "Field Evaluation Of The Differential TEOM® Monitor By Comparison With Semi-continuous And Integrated Ambient Particulate Mass And Nitrate In Claremont, California" Submitted to *Aerosol Science and Technology*, October 2002

16. Bhabesh Chakrabarti, Manisha Singh and Constantinos Sioutas "Development of a Near-Continuous Monitor for Measurement of the Ultrafine PM Mass Concentration" Submitted to *Aerosol Science and Technology*, October 2002

17. Yifang Zhu, , William C. Hinds, Si Shen, and Constantinos Sioutas "Seasonal Trends of Concentration and Size Distributions of Ultrafine Particles Near Major Freeways in Los Angeles". Submitted to *Aerosol Science and Technology*, October 2002

18. Li, N., Sioutas, C , Froines, J.R., Cho, A., Misra, C and Nel, A., "Ultrafine Particulate Pollutants Induce Oxidative Stress and Mitochondrial Damage" *Environmental Health Perspectives*, in press, December 2002

3. PIU Sampling Location and Status

During the period of this progress report, we began PM sampling with the Particle Instrumentation Unit (PIU) at the University of Southern California (USC), the fifth Southern California Supersite location, beginning September 2002. The site is located about one mile directly south of downtown Los Angeles and the 10 Freeway, which runs east to west, and is about 100 meters directly east of the 110 Freeway. The site is embellished with typical urban sources: centralized within a major congested urban center; adjacent to several 2 – 7 story buildings; adjacent to pedestrian and local traffic as well as central arteries; and near building and road construction projects. Since the site is about 15 miles directly east of the ocean, prevailing winds are primarily from the west during most of the daytime when mobile and stationary emission sources may be expected to predominate. However, the nearby relatively large buildings can also disturb the winds resulting in an urban canyon effect, causing turbulence and wake effects that may increase the delivery of other local sources (e.g., construction debris, and larger settled particles from road related vehicle wear-and-tear) in addition to the close-by 110 Freeway. Several studies are being conducted as we enter the 2nd quarter at the USC site to investigate local source contributions in addition to the regional transported emissions that may generally come from the west freeways.

We have completed all chemical speciation analysis for integrated samples, through most of November, and have continued to make size integrated on-line measurements of particulate nitrate and carbon using the Integrated Collection and Vaporization System (ICVS) developed by Aerosol Dynamics Inc. Semi-continuous PM2.5 measurements continue to be made with a set of prototype Differential TEOMs, designed to measure "non-artifact" laden mass. Two continuous BAM monitors have been operating: one, with the standard PM2.5 inlet, the second with an ultrafine concentrator inlet (designed at our USC lab). Coupled with our USC-TEOM coarse monitor, time-integrated mass measurements are being compared to those by our SMPS-APS and Differential ESP TEOM for short term periods, and to MOUDI, Partisol, and other filter mass samplers for longer sample integrals, overall, resulting in paired integrated semi-continuous, diurnal, and 24-hour mass measurements of coarse, fine, and ultrafine PM.

Additionally, we have continued to make our mobile particle trailer available for co-located exposure studies. The following health studies have been supported by the Supersite measurements: In vitro studies undertaken by Drs. Andre Nel and Arthur Cho (UCLA) investigating the hypotheses that organic constituents associated with PM, including quinines, other organic compounds (PAHs, nitro-PAHs, and aldehydes/ketones) and metals are capable of generating reactive oxygen species (ROS) and acting as electrophillic agents. These are ongoing studies. Animal inhalation toxicology studies using Concentrated Ambient Particulates (CAP) investigating the hypotheses that atmospheric chemistry is important in the toxicity of PM and co-pollutants, airway injury and cardiovascular effects will be greater at receptor sites downwind of source sites along the mobile source trajectory in the Los Angeles basin. Led by Drs. Harkema (University of Michigan), Kleinman (UC Irvine), Froines, and Nel (UCLA), these co-located studies have commenced during our first month at the USC site. Additionally, as with Claremont, exposure studies will continue throughout this winter to investigate seasonal changes in toxicity near this urban site.

4. Time Integrated Size Fractioned Chemical Speciation for Claremont

Introduction

Our current sampling scheme continues to involve the use of three MOUDI for 24-hour averages: size-fractionated measurements of ambient and concentrated PM mass and chemical composition. Additionally, a Partisol is used to acquire the coarse fraction of mass. Sampling is conducted once a week, typically on Tuesday, Wednesday or Thursday. However, this schedule is flexible to be adjusted for our "intensive" particulate characterization studies and/or for our support of co-located health effects exposure studies. Typically, ambient data are averaged over 24 hours (midnight to midnight), whereas for exposure or source contribution measurements, the time integrals may vary. Except for special studies that may involve3 other size cuts, consistent with our original Supersite proposal, we have used three collocated Micro-Orifice Uniform Deposit Impactors (MOUDI) to generate five PM size ranges:

<0.1 μm	(ultrafine particles)
0.1- 0.32 μm	(accumulation mode, "condensation" sub-mode)
0.32 – 1.0 μm	(accumulation mode, "droplet" sub-mode)
1.0 – 2.5	("intermediate" mode)
2.5-10 μm	(coarse particles)

In addition to mass concentration, the following chemical components have been analyzed within these size groups: inorganic ions (i.e., sulfate, nitrate, ammonium), analyzed by ion chromatography (Dionex); trace elements and metals, analyzed by XRF; and the elemental and organic carbon (EC/OC) content is analyzed by thermal optical detection. For USC, sample analysis is complete through about mid November for chemical data, and mid December for mass. Mass and chemical size fractionated data are presented for the USC site; and, for continuity averaged data is compared to that of Claremont.

Results

Figure 1 presents 24 hour averaged size segregated mass. The results show that, on the average, the coarse and fine fractions are about equivalent, between about 22 and 25-μg/m3. The "droplet" sub-mode predominates at about 11 μg/m3, nearly twice as great as the adjacent modes. The site is about 100 meters downwind of the 110 freeway On-Ramp. It is expected to receive freshly generated mobile source PM (e.g., Zhu, et al., 2002), but may be confounded by local coarse particles that could come from vehicle-to-road wear-and-tear, as well as local construction debris, all re-suspended via the urban canyon wake effect.

Figure 2 presents diurnal mass results of a 1-week intensive study, similarly showing that the droplet mode tends to predominate, along with the intermediate mode; and, is greater during the morning a and noon rush hours. Local construction emissions may add to these two periods, as this is the work period, which ends sometime about 4pm, and would less so, contribute to the 2-6pm period.

Figure 3 presents size segregated 24hour NH4NO3 and (NH4)2SO4, while Figure 4 presents that for EC and OC. PM 2.5 mass predominates for all species. The droplet mode for NO3, SO4, and OC dominates in the Fine fraction, while the ultrafine mode (<0.1 um) does for EC, which suggests local mobile source emissions. However, the local construction may add to this mass when using combustion related equipment. Generally, this speciated data corresponds with the mass measurements.

Figures 5 and 6 present size segregated mass and relative-mass Anthropogenic and Crustal speciated source metal elements. In general the Anthropogenic metals are higher in the coarse fraction, although relatively high in the Fine fractions for Vanadium, Chromium, Zinc, and Copper, and not present in the coarse for Nickel, suggesting non-Crustal sources. The crustal metal elements clearly predominate in the coarse mode, and account for about 10% of the intermediate mode.

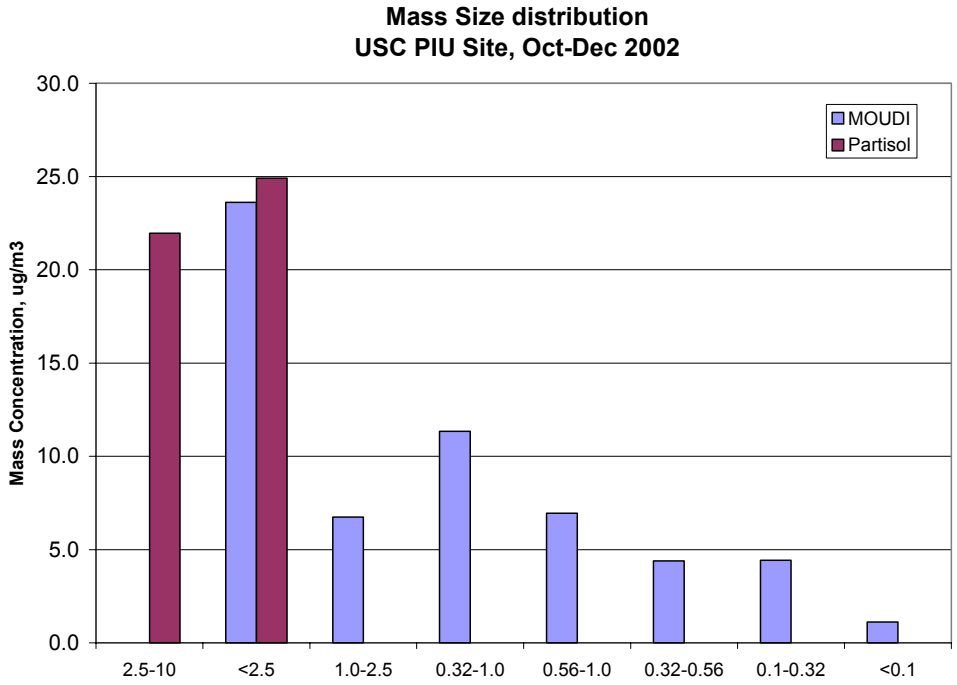

Figure 1. Mean (N=8) MOUDI size fractionated measurements of ammonium nitrate and Sulfate at USC PIU site for October through early December, 2002.

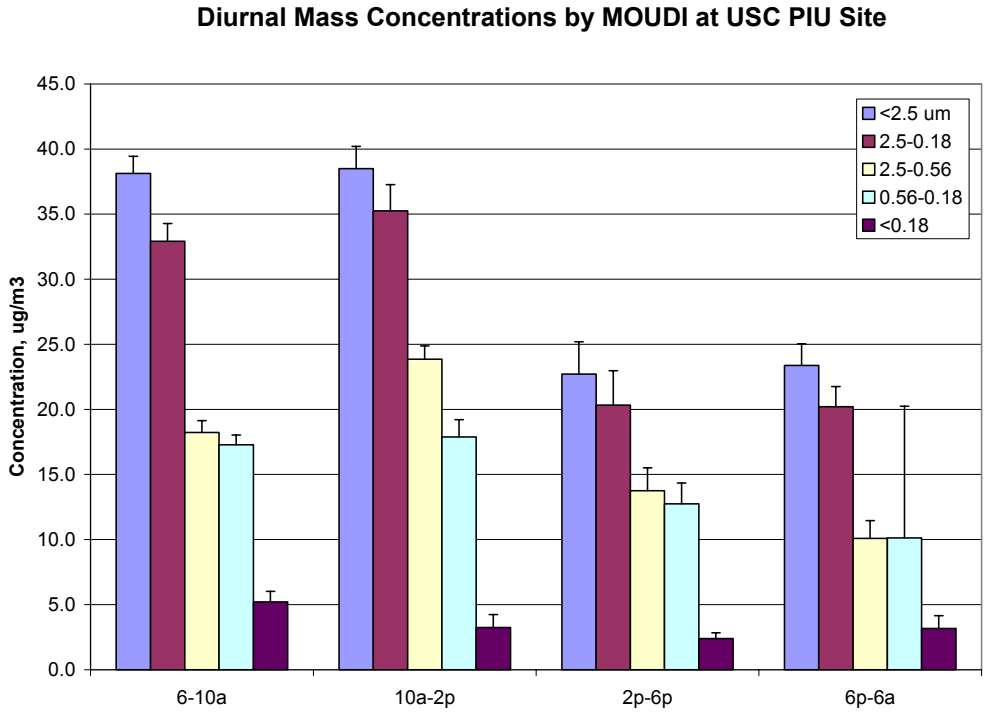

Figure 2. Diurnal size fractionated PM mass for a one-week intensive study at USC PIU site during the 2nd and 3rd week of December 2002.

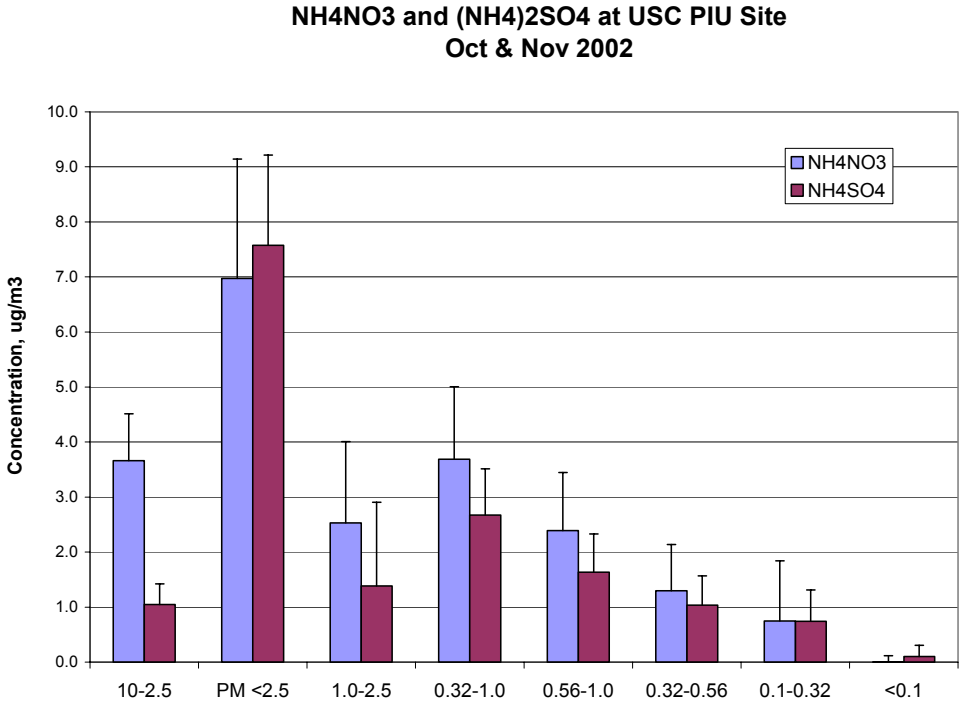

Figure 3. Mean (N=6) MOUDI size fractionated measurements of ammonium nitrate and Sulfate at USC PIU site for October and November, 2002.

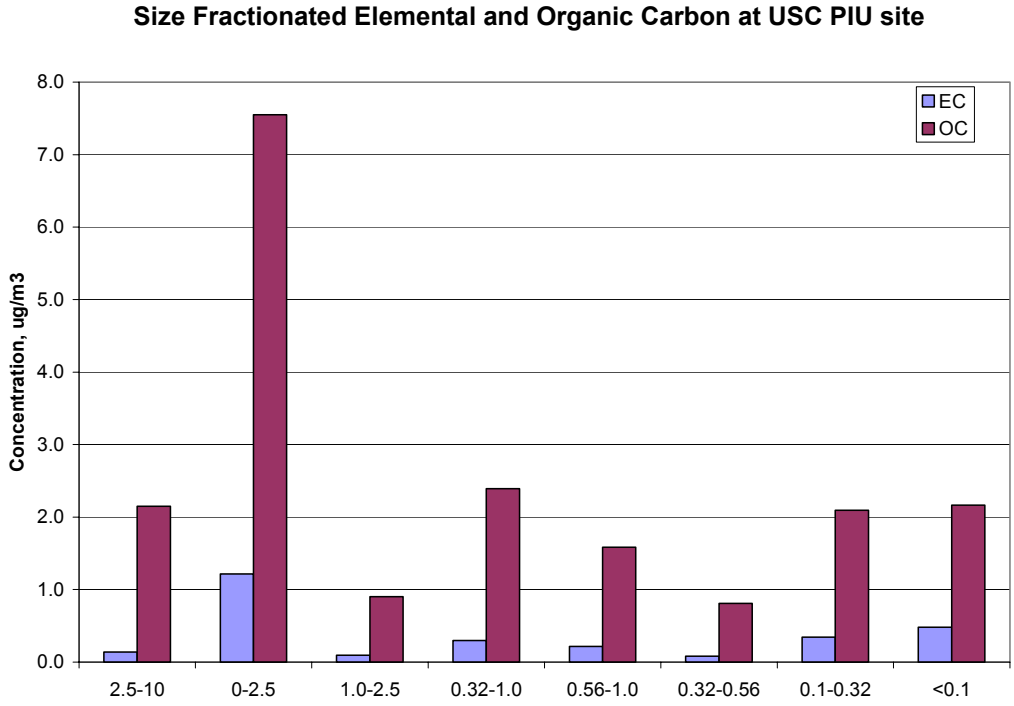

Figure 4. Mean (N=7) MOUDI size fractionated measurements of Elemental and Organic Carbon at USC PIU site for October and November, 2002.

a)

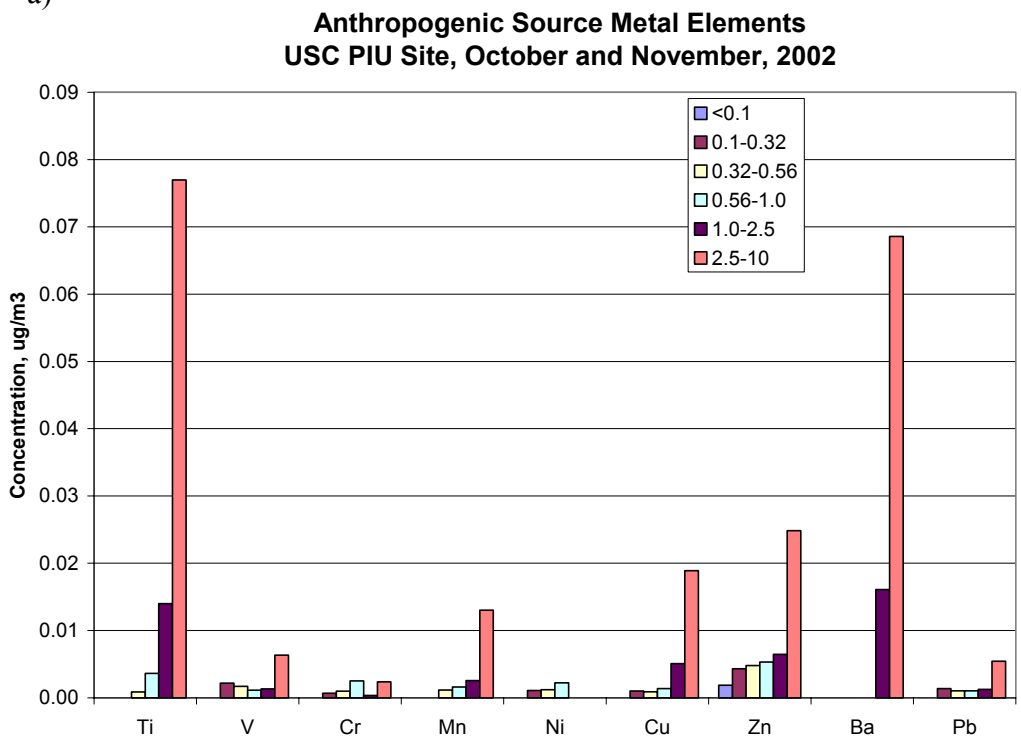
Anthropogenic Source Metal Elements
USC PIU Site, October and November, 2002
Concentration, ug/m3
0.09
0.08
0.07
0.06
0.05
0.04
0.03
0.02
0.01
0.00
<0.1
0.1-0.32
0.32-0.56
0.56-1.0
1.0-2.5
2.5-10
Ti
V
Cr
Mn
Ni
Cu
Zn
Ba
Pb

b)

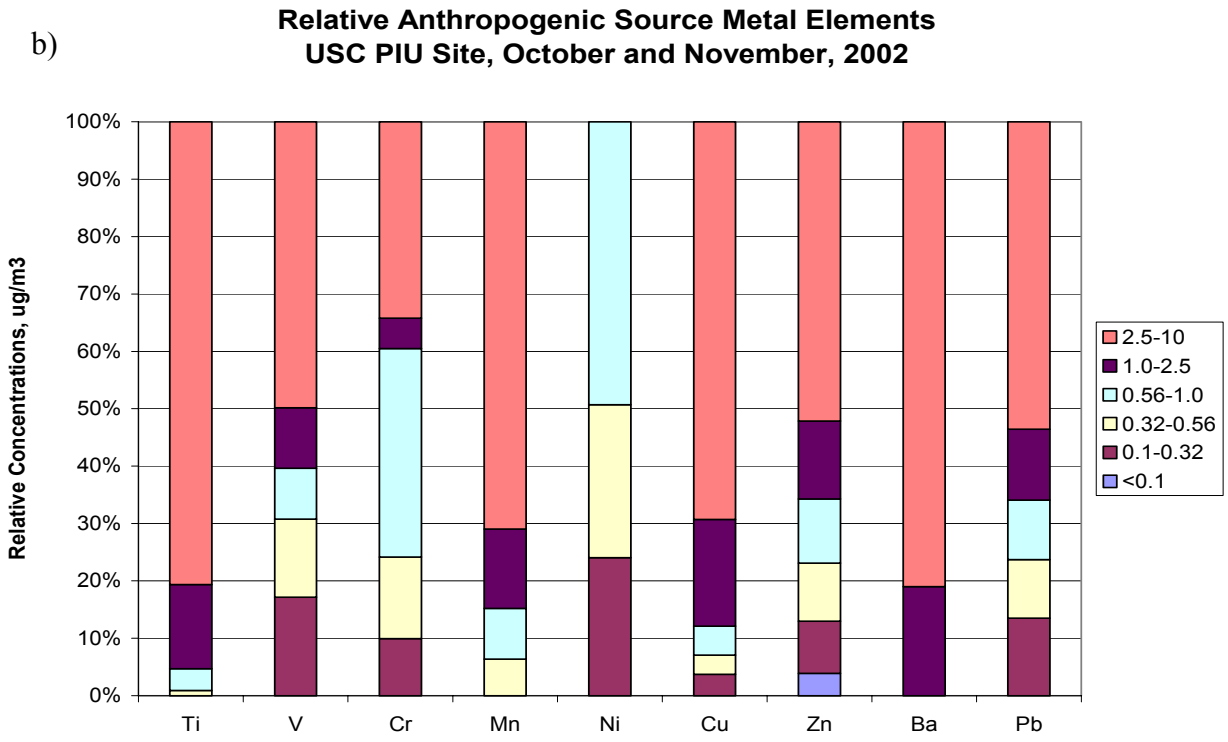

Figure 5. a) Concentration & b) Relative Concentration of Metal Elements typically found in anthropogenic sources.

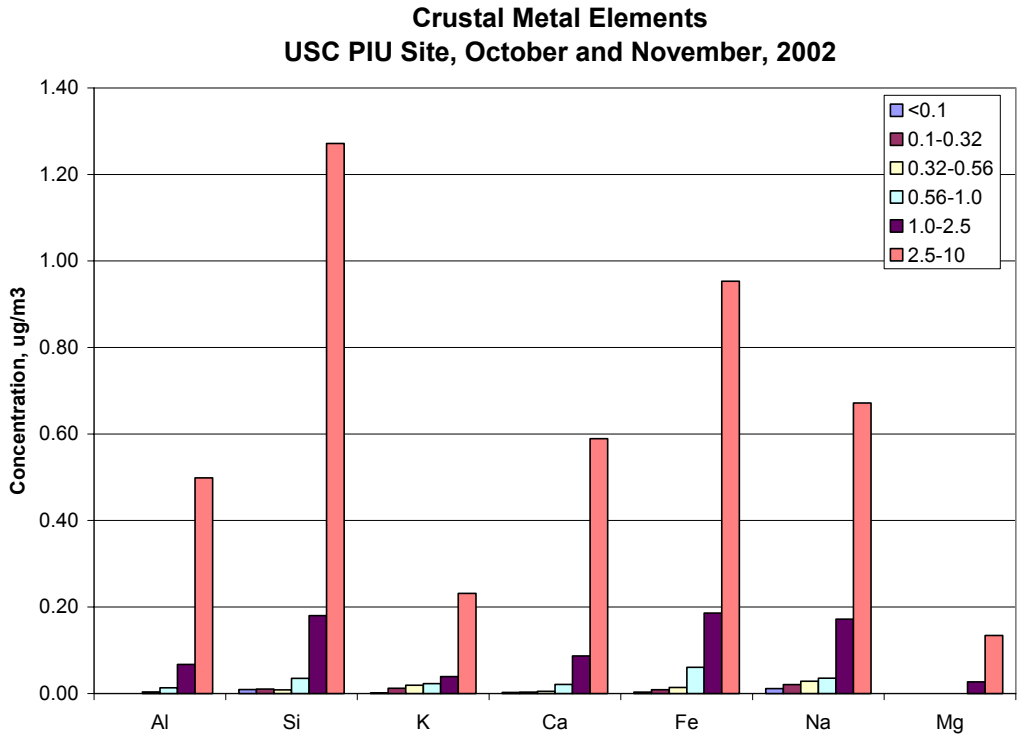

b)

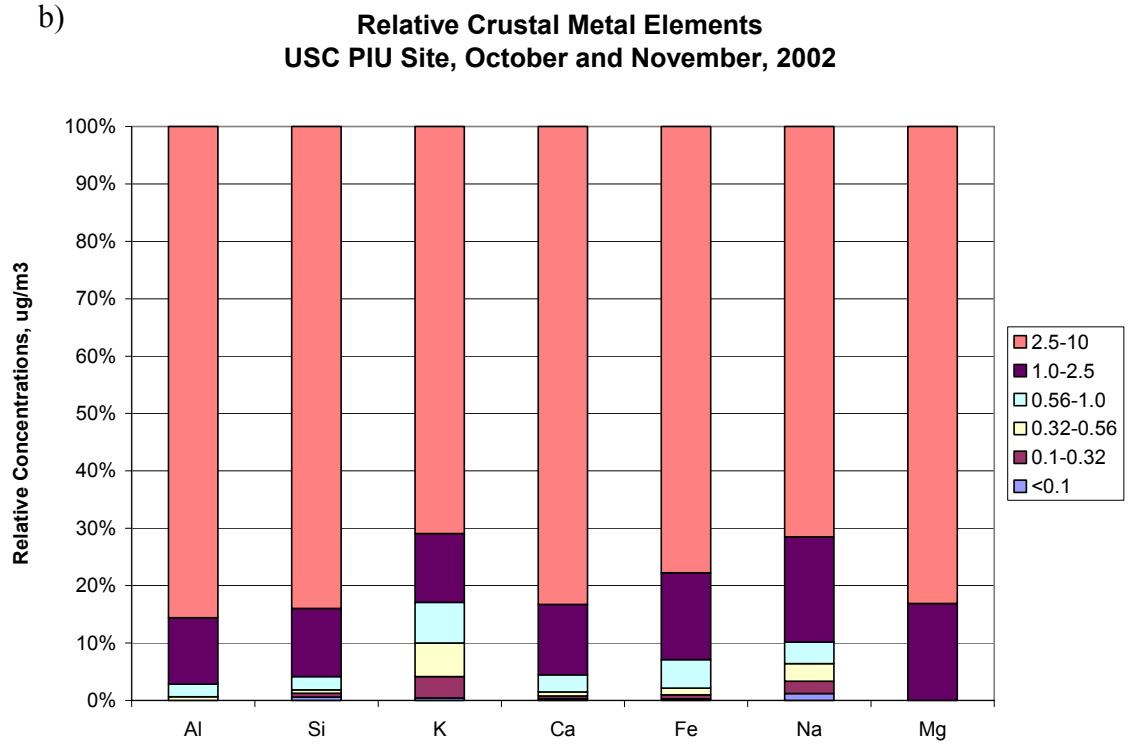

Figure 6. a) Concentration & b) Relative Concentration of Metal Elements typically found in sources.

5. Inferring the Sources of Fine and Ultrafine Particulate Matter at Downwind Receptor Sites in the Los Angeles Basin Using Multiple Continuous Measurements

An analysis of SMPS-APS and aethalometer data collected by the Particle Instrumentation Unit was completed this quarter. A paper with the above name was submitted for publication to a special issue of Aerosol Science and Technology dedicated to the Supersite program. The following is a brief summary of the results and analysis included in that manuscript.

Recent studies that have found increased health effects of atmospheric ultrafine particulate matter (PM) have refocused attention on particle number rather than particle mass concentrations as a relevant measurement of PM pollution. For this study, ambient particle characteristics were measured over 13 months at three different sites in the eastern portion of the Los Angeles Basin: Riverside, Rubidoux and Claremont, CA. The sites represent receptor locations that are influenced by local particle sources as well as advection from the more intense particle sources upwind closer to Downtown Los Angeles. An SMPS/APS tandem system was employed to collect continuous particle size distributions, from which particle number and mass concentrations were calculated. An aethalometer provided continuous particulate elemental carbon (EC) concentrations.

The following figure displays the relationship between $PM_{2.5}$ mass and number as measured by the SMPS-APS system over the period studied. Particle mass was calculated based on the size distribution assuming a particle density of 1.6 g/cm^3. Results show no meaningful correlation between particle number and mass, indicating that fine particle standards may not be effective in controlling particle number, and therefore ultrafine particle, concentrations.

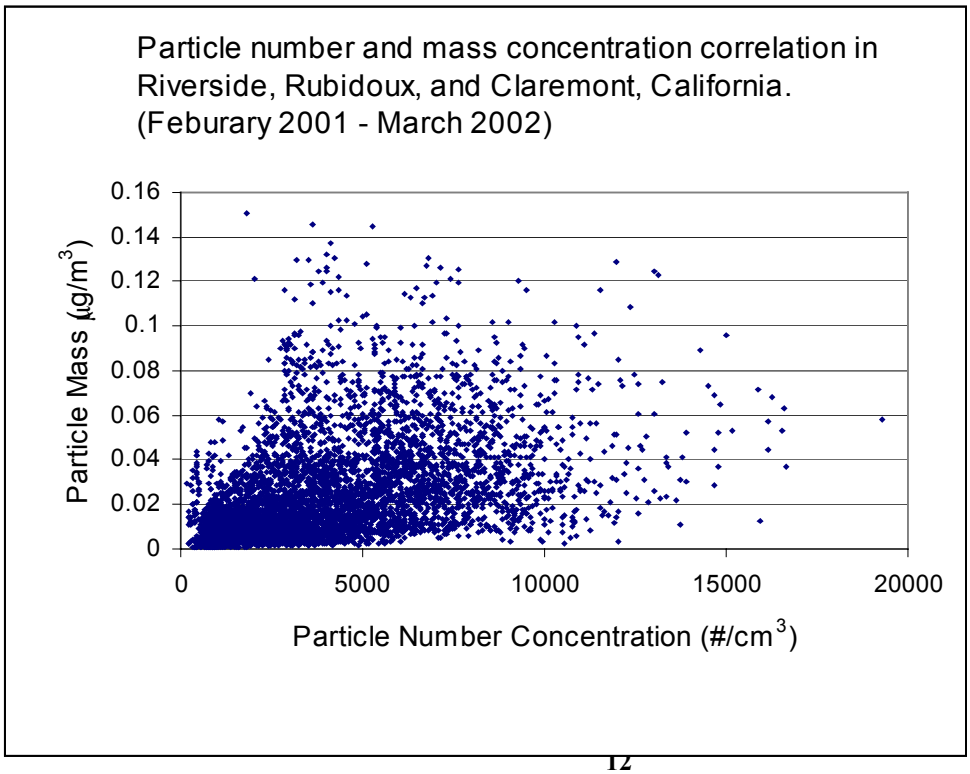

The following two figures show the monthly average EC, particle number and particle mass concentrations on an hourly basis. The first set of figures displays results from Riverside and the second set shows results from Claremont. At both sites, diurnal patterns include a morning traffic peak indicated by increases in particle mass, number, and EC. Afternoon periods in the warmer months are characterized by high number counts while mass and EC remain low, suggesting the formation of new particles by photochemistry. While particle nucleation was not directly observed, the other possible causes of an increase in particle number can be discounted. Low EC levels indicate that vehicular emissions do not cause the afternoon increase in particle numbers. The inversion height increases in the afternoon. And the particle size mode in the afternoon is smaller than in the morning indicating that the aerosol has not grown during transport from urban sources upwind.

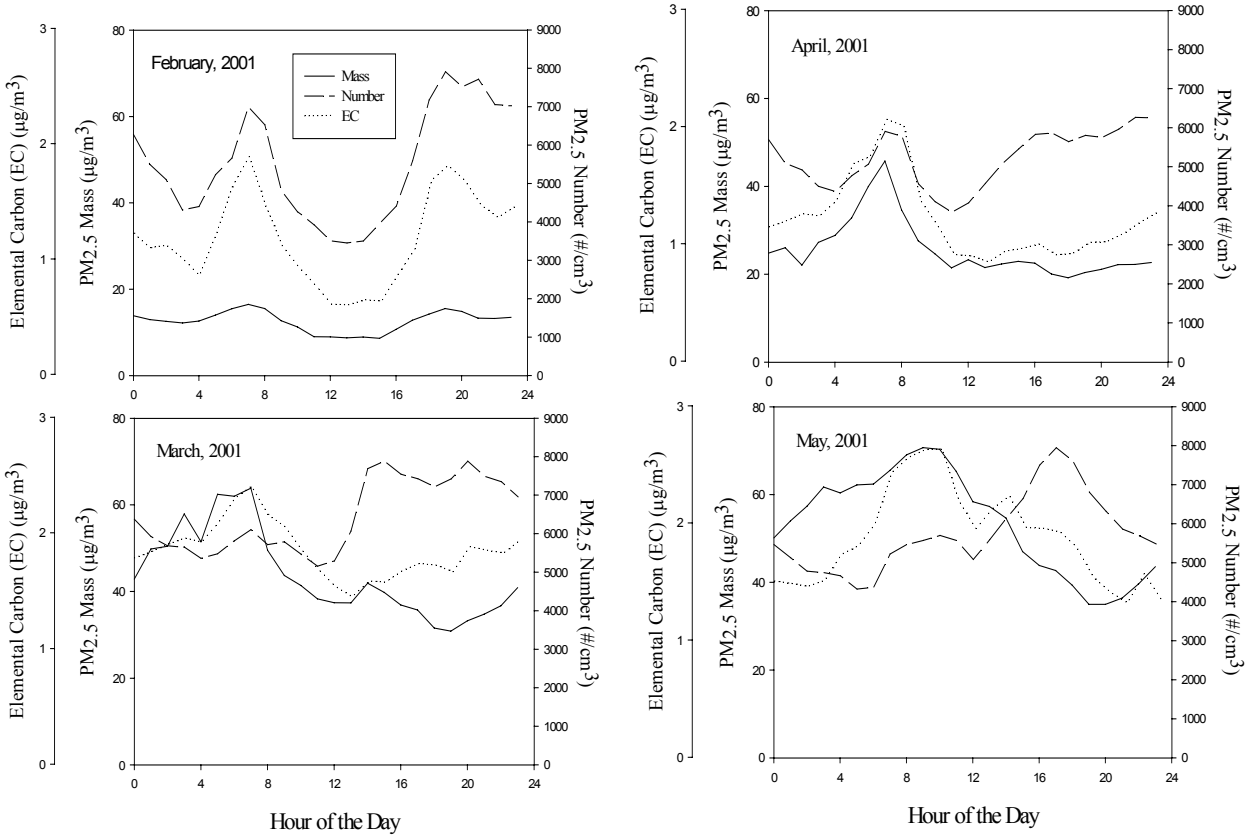

Figure 4. Diurnal profile of $PM_{2.5}$ particle number, mass and elemental carbon mass concentration in Riverside, California.

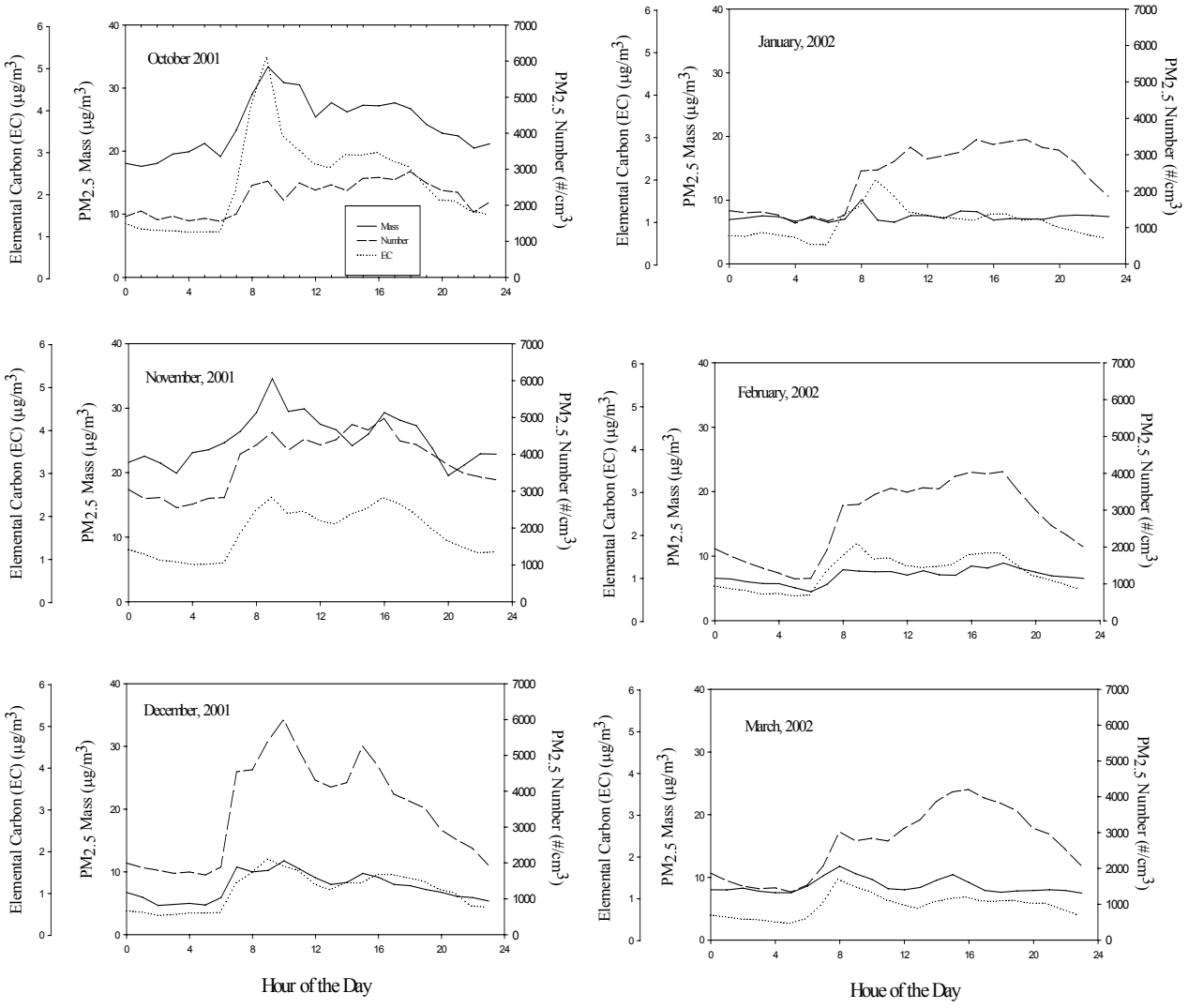

Figure 10. Diurnal profile of $PM_{2.5}$ particle number, mass concentration and elemental carbon mass concentration in Claremont, California.

The following figure shows the lower particle mode diameters observed in the afternoon at the Rubidoux site. Particle mode diameters range from 40 nm up to above 100 nm, a result not seen in most other studies of particle size distributions in other urban or rural areas where mode diameters are generally less than 50 nm.

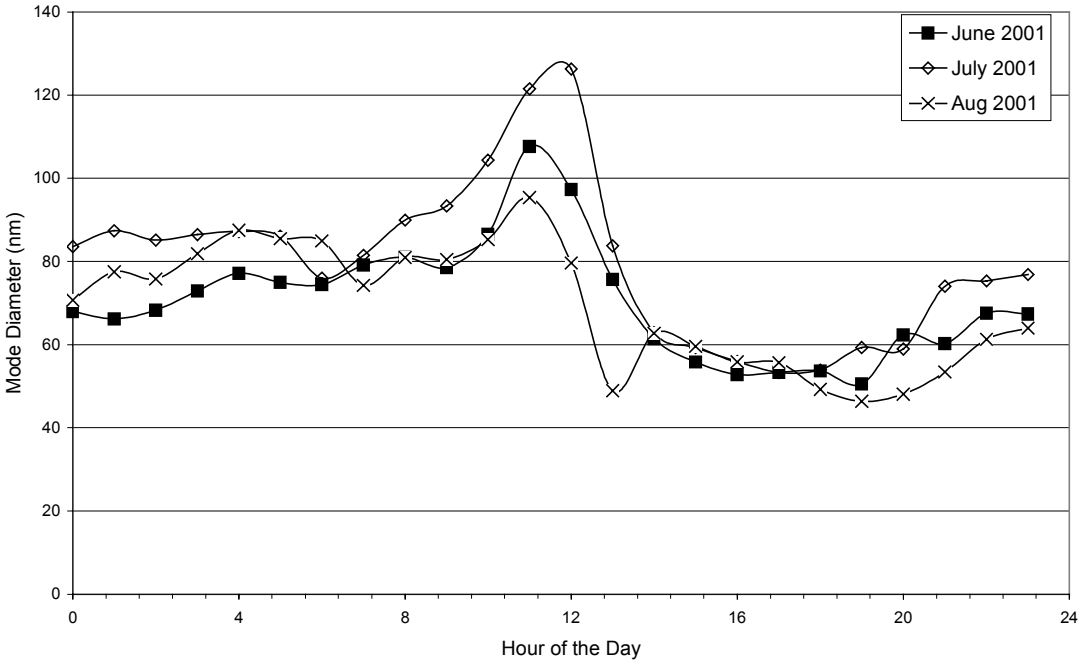

Figure 8. Monthly averaged mode diameter in Rubidoux, California.

The next figure gives representative size distributions over the course of a typical day in Riverside. Note the appearance of a second smaller mode by 6PM that diminishes overnight. The larger, more persistent mode is due to advection and atmospheric growth of particles emitted upwind in the western portion of the LA Basin. The smaller mode which only is observed in the afternoon and during the warmer months is presumably due to atmospheric formation of new particles.

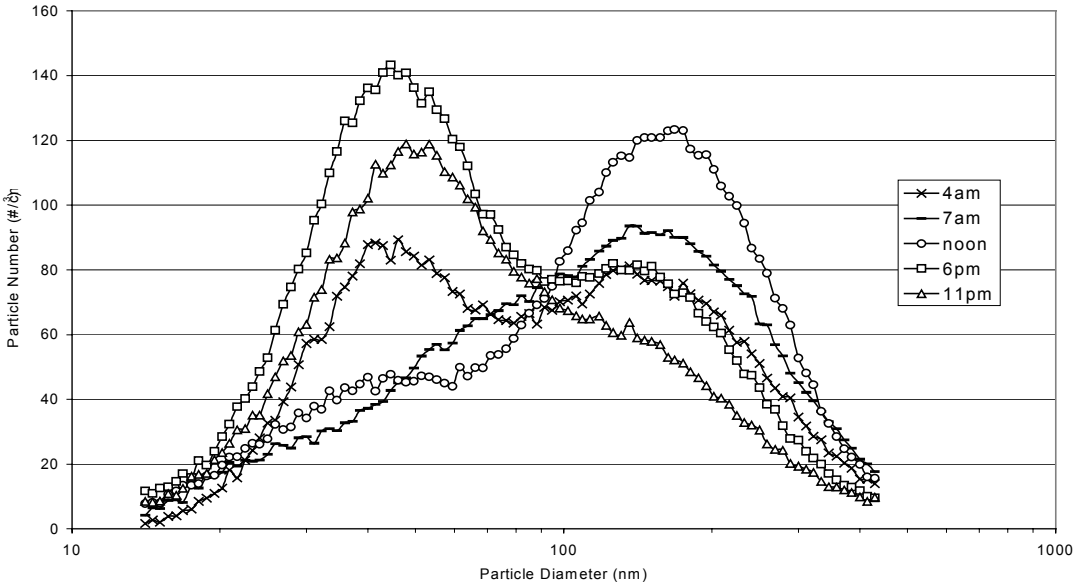

Figure 7. Size distribution in Riverside, California, (May 16, 2001).

6. Predicting Ultrafine Particles near Major Freeways

Recent toxicology studies have implicated atmospheric ultrafine particles (diameter < 100 nm) for some of the adverse effects observed due to exposure to atmospheric particulate matter (PM) concentration (Ferin et al., 1990). In an urban environment motor vehicle emissions usually constitute the most significant source of ultrafine particles. However, there is very little information available either as to the size of the particles or as to the number concentration of ultrafine particles emitted by vehicles.

The present research focuses on developing a model to determine ultrafine particle behavior after emissions, as they are transported away from the emission source --- a freeway. The overall goal of this research is to test two hypotheses. First, that a physical model can predict the changes in size distribution and number concentration of ultrafine particles as they are carried away from a freeway by the wind. Second, that ambient ultrafine particle concentration adjacent to a freeway can be predicted from traffic density and speed together with meteorological factors. In other words, ultrafine particle concentration at a certain distance from a freeway can be predicted quantitatively.

Previously we have completed experimental measurements of ultrafine particle number concentration and size distribution near two freeways in summer and in winter (Zhu et al. 2002a; Zhu et al. 2002b). Results from these studies are used to validate model prediction.

As a first step to modeling the concentration and size distribution of ultrafine particles in the vicinity of freeways, atmospheric dispersion model was developed based on Carbon Monoxide (CO) data that we collected during our previous field studies. Since vehicular exhaust emission on the freeways is the major concern in the model, a line source emission model was adopted.

The most commonly used line source Gaussian Plume model, is based on the superposition principle, namely concentration at a receptor, which is the sum of concentrations from all the independent infinitesimal point source making up a line source. It also assumes the emission from a point source spreading in the atmosphere in the form of plume, whose concentration profile is generally Gaussian in both horizontal and vertical directions. The concentrations downwind of a continuously emitting infinite line source, when the wind direction is normal to the line, is given by

$$C(x,z) = \frac{q_l}{U\sigma_z\sqrt{2\pi}}\left\{\exp\left(-\frac{(h-z)^2}{2\sigma_z^{\,2}}\right)+\exp\left(-\frac{(h+z)^2}{2\sigma_z^{\,2}}\right)\right\} \qquad (1)$$

where $C(x,z)$ is the pollutant concentration at the receptor, q_l is the source strength, U is wind speed, σ_z is vertical dispersion parameter, h is emission height, z is the sampling height, x is the downwind distance. The vertical dispersion parameter is a function of Pasquill stability class and downwind distance from the source. Under the experimental conditions that we had, σ_z can be expressed as

$$\sigma_z = a \times x^b \qquad (2)$$

with a equal to 122.8, and b equal to 0.9447 (Turner 1994).

The US Environmental Protection Agency and many other research institutes have developed a number of line source models for estimating vehicular pollutant concentrations. Among them, CALINE4, developed by the California Department of Transportation (Caltrans), requires relatively minimal input from the user and is chosen here for comparison. CALINE4 is also based on the Gaussian diffusion equation but employs a mixing zone concept to characterize pollutant dispersion over the roadway.

While Gaussian model has been widely used to simulate atmospheric dispersion, many researchers have found that the Gaussian distribution does not represent well the pollutant concentration distribution under strong convective situation and ground-level release (Seinfeld and Pandis 1998; Sharan et al. 1996; Turner 1994). Instead, the atmospheric diffusion equation was found to provide a more general approach than the Gaussian models. Under the assumption of incompressible flow, atmospheric diffusion equation based on the Gradient-transport theory (K-theory) in the absence of chemical reaction is

$$\frac{\partial C}{\partial t}+u\frac{\partial C}{\partial x}+v\frac{\partial C}{\partial y}+w\frac{\partial C}{\partial z}=\frac{\partial}{\partial x}\left(K_{xx}\frac{\partial C}{\partial x}\right)+\frac{\partial}{\partial y}\left(K_{yy}\frac{\partial C}{\partial y}\right)+\frac{\partial}{\partial z}\left(K_{zz}\frac{\partial C}{\partial z}\right) \qquad (3)$$

where C is the mean concentration of a pollutant; (u, v, w) and (K_{xx}, K_{yy}, K_{zz}) are the components of wind and eddy diffusivities vectors in x, y and z direction, respectively, in an Eulerian frame of reference.

For a continuous, crosswind line source ($\partial C/\partial y = 0$), at a height h emitting at a rate q_l (g m^{-1} s^{-1}), with following assumptions

(a) Steady-state conditions, i.e. $\partial C/\partial t = 0$.
(b) The vertical velocity is much smaller than the horizontal one so that the term $w(\partial C/\partial z)$ is neglected.
(c) x-axis is oriented in the direction of mean wind, i.e. $u = U$ and v=0, where U is a non-zero constant.
(d) The diffusion in the direction of the mean wind is neglected, i.e. $K_{xx} = 0$.

Equation (3) reduces to

$$U\frac{\partial C}{\partial x}=\frac{\partial}{\partial z}\left(K_{zz}\frac{\partial C}{\partial z}\right) \qquad (4)$$

The source term q_l is introduced through the following boundary conditions;

$$C\,(0,z) = (q_l/U\,(\mathrm{h}))\,\delta(\mathrm{z\text{-}h}) \qquad (5)$$

Where δ (.) is Dirac's delta function.

Far away from the line source, the concentration decreases to zero, i.e.

$$C(x,z)=0 \qquad x,z\to\infty \qquad (6)$$

Ground surface is assumed impermeable to the pollutants, i.e.

$$\frac{\partial C}{\partial z}=0 \qquad \text{at z = 0} \qquad (7)$$

For near source diffusion, Sharan et al., (1996) showed that *K*s, the eddy diffusivities, can be specified as linear functions of downwind distance based on (Taylor 1921) statistical theory of diffusion for smaller travel times. Thus,

$$K_{zz} = \gamma U x \qquad (8)$$

where γ represents turbulent parameter in the z direction and varies with atmospheric stability. Now equation (4) becomes

$$\frac{\partial C}{\partial x}=\gamma x\frac{\partial^2 C}{\partial z^2} \qquad (9)$$

Equation (9) with boundary conditions (5), (6) and (7) can be solved analytically using Fourier's transforms or similarity method to obtain

$$C(x,z)=\frac{q_l}{U x\sqrt{2\gamma\pi}}\left\{\exp\left(-\frac{(h-z)^2}{2\gamma x^2}\right)+\exp\left(-\frac{(h+z)^2}{2\gamma x^2}\right)\right\} \qquad (10)$$

For practical application, the turbulence parameter γ, can be identified as the square of turbulence intensity using Taylor's statistical theory of diffusion, i.e.

$$\gamma=\left(\frac{\sigma_w}{U}\right)^2 \qquad (11)$$

When the measurements of turbulence intensities are available, γ should be computed directly. In the absence of direct measurement, mixed-layer similarity scaling and empirical turbulence data suggest that $\sigma_w = b\, w_*$, where w_* is the convective velocity scale. Depending on the dimensionless height z/z_i, where z_i is the convective mixing height, the constant b can be from 0.4 to 0.6. It is a good approximation to take b=0.4 for modelling dispersion in the surface layer and b=0.6 in the mixed layer. Thus, turbulence parameter can be expressed as

$$\gamma = 0.16(w_*/U)^2 \qquad (12)$$

Figure 1 compares experimental CO concentration data that we obtained near the 405 freeway (Zhu et al., 2002a) with model predictions. A common Gaussian Plume model, the CALINE4 model and the K-theory model, developed in this study, were included in Figure 1. For all three models, the emission height has been set to the height of the freeway, 4.5 m; sampling height is 1.6 m. Source strength q_l is 0.0314 gram/sec/m which equivalents to a traffic density of 14,000 vehicle per hour with emission factor of 13 gram/mile. Wind speed is 1.5 m/s perpendicular to the freeway. All of these three models predict a sharp increase close to the source due to the difference between the source and receptor height and an exponential decay as moving away from the source. The K-theory we developed predicts a sharper decay, which fits best to the experimental data. Figure 2 compares vertical CO concentration that we measured near the 405 freeway in summer 2001 with model predictions. Again, K-theory with eddy diffusivities as a linear function of downwind distance gives the best fit.

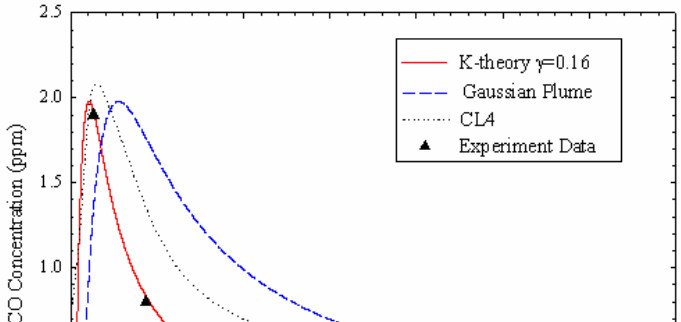

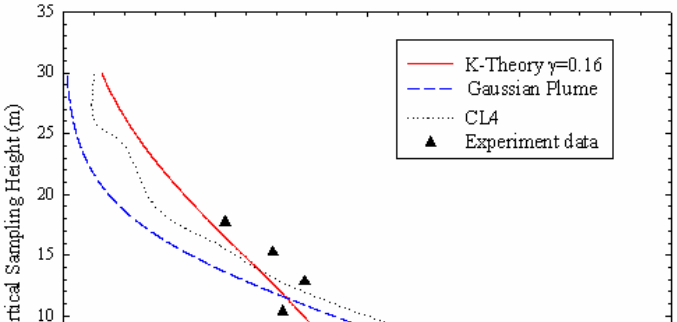

Figure 1. Comparison of CO concentrations predicted by different modals with experiment . data.

Figure 2. Comparison of vertical CO concentration predicted by different modals with experiment data.

References:

Ferin, J.; Oberdörster, G.; Penney, D.P.; Soderholm, S.C.; Gelein, R. and Piper, H.C., Increased pulmonary toxicity of ultrafine particles? I. Particle clearance, translocation, morphology. *J. Aerosol Sci*. 1990; 21: 384-387.

Seinfeld, J. H. and Pandis, S. N. (1998). Atmospheric Chemistry and Physics: from Air Pollution to Climate Change. Wiley, New York.

Sharan, M., Singh, M. P. and Yadav, A. K. (1996). Mathematical model for atmospheric dispersion in low winds with eddy diffusivities as linear functions of downwind distance *Atmospheric Environment*. 30:1137-1145.

Taylor, G. I. (1921). Diffusion by continuous movements *Proceedings of London Mathematical Society*. Ser. 2XX:196-212.

Turner, D. B. (1994). Workbook of Atmospheric Dispersion Estimates: An Introduction of Dispersion Modeling, 2nd edition 2-11.

Zhu, Y., Hinds, W. C., Kim, S., Shen, S. and Sioutas, C. (2002b). Study of Ultrafine Particles near a Major Highway with Heavy-duty Diesel Traffic. *Atmospheric Environment*. 36:4323-4335.

Zhu, Y., Hinds, W. C., Kim, S. and Sioutas, C. (2002a). Concentration and Size Distribution of Ultrafine Particles near a Major Highway. *Journal of Air and Waste Management Assoc.* 52:174-185.

7. Ultrafine Organic Speciation Study

Several studies have measured individual organic compounds in atmospheric particle samples by GC/MS or other analytical methods. Usually only between 10 and 20% of the total organic compound mass (measured by thermal desorption methods) can be quantified as individual organic species. Some of these compounds can be used to trace primary particle emissions and be used in source apportionment studies. One of the major hurdles in the sampling of particles for organic speciation is collecting enough mass for the analysis. For this reason, sampling periods are very long (from 12 hours to several days) and they do not provide size-fractionated information on the organic particle concentrations. The one study that measured size-fractionated speciated organics only looked at PAH and oxy-PAH and sampled over 5 - 24 hour periods (J. Allen et al., 1996,1997, 1998).

A new particle slit impactor developed by Dr. Sioutas and his group (Misra et al., 2002) through funding by the Southern California Supersite enables the separation of particles with a cut point of 0.18 μm and a very high flow rate of ~500 lpm. Using a 2.5 μm inlet, particles with diameters between 0.18 μm and 2.5 μm (fine) can be collected by impaction on this new impactor, and particles with diameters less than 0.18 μm (ultrafine) can be collected on a high-volume filter downstream. The two size fractions roughly correspond to the accumulation mode and ultrafine modes of the urban aerosol size distribution. The high flow rate of the system allows for shorter collection periods, and thus diurnal (3 ½ - hour samples) and size-segregated sampling for organic speciation is now possible.

The sampling plan is outlined below. Briefly, two sampling sites were selected: a typical urban site (USC); and a downwind receptor site (Riverside). For one week at each site (Mon. – Fri.), four time intervals per day are sampled (morning, midday, evening, and possibly overnight). The daytime samples last 3 1/2 hours per day for each diurnal interval for five days. Nighttime sampling lasts for 11 1/2 hours per night for four nights. Filters and substrates are replaced in the sampler such that one set of accumulation mode quartz-fiber substrates and one ultrafine mode high-volume Teflon-coated glass fiber filter represent a weekly average for each diurnal interval. Parallel to the high volume sampler will be a MOUDI run at 30 lpm to collect particles on Teflon substrates for mass and potentially ion chromatography and ICP/MS analysis in the future. The stages in the MOUDI will be chosen to correspond to the same cut-points as the high volume sampler. A second MOUDI with the same flow rates and size cuts will collect aluminum foil substrates and a quartz fiber after filter for EC/OC analysis by the thermal desorption/optical transmission method used regularly by the Supersite. In addition, a 47mm filter train will consist of a PM2.5 inlet, a Teflon filter and a back-up quartz fiber filter. The flow rate will be chosen to create a face velocity on the quartz back-up filter equal to the face velocity on the MOUDI quartz after filter. This filter-based sampling helps to assess the degree of organic vapor adsorption onto the MOUDI quartz after filter.

An additional high volume sampling system, operated by Dr. Janet Arey's UCR group, will consist of a filter followed by a PUF and will be used for analysis of both semi-volatile and particle-phase PAH, oxy-PAH and nitro-PAH.

A fifth system, consisting of a nano-MOUDI running at 10 lpm, will be used to collect samples at each site for ultrafine, size-segregated, PAH and quinone analysis by Tony Miguel. In order to collect sufficient mass, the nano-MOUDI runs for full 11 1/2 hour daytime and nighttime periods that correspond to the three daytime and nighttime intervals of the other samplers.

The purpose of this project is several-fold. First, with the exception of the one study on PAH and oxy-PAH, the speciated organic composition of ultrafine particles has not been investigated. Several other classes of compounds, including alkanes, substituted phenols, alkenes, alkanoic acids and diacids, aromatic carboxylic acids, resin acids, sugars and furans have been found in atmospheric particles but their distribution among size fractions is unknown. Ultrafine particles consist of fresh particles emitted directly from sources, freshly condensed material on these primary particles, and freshly nucleated particles resulting from atmospheric reactions. It has also been shown that ultrafine particles consist of up to 80% - 90% organic carbon. Source profiles for many of the organic compounds of interest have been previously determined for the most important particle sources in Los Angeles (Schauer Thesis, 1998). Furthermore, smog chamber studies have identified many particle phase organic atmospheric reaction products that should also be found in the atmosphere.

By comparing individual ultrafine organic species to known organic source profiles and expected atmospheric reaction products, the sources and formation mechanisms of these ultrafine particles can be determined. Recent data suggesting that ultrafine particles may be more toxicologically potent than larger particles provide even more motivation for this study. First identifying the origin, the geographical distribution, and the diurnal and seasonal variations of these particles will help to model personal exposure and to formulate any future pollution control efforts. Second, the toxicological effects of the ultrafine aerosol as a whole can be compared to the toxicity of the identified organic components. The sampler can also be used to collect extra ultrafine material for subsequent toxicity assays performed by Drs. Nel and Cho at UCLA.

By also looking at the organics on the accumulation-mode filter sample, the contributions of primary particle sources and secondary organic aerosol to the two particle size fractions can be resolved over the course of the day and as air parcels move across the LA basin. The organic components of the accumulation-mode particles will also have toxicological implications, and can be compared to the organic components found in the ultrafine fraction.

Finally, the warm weather and large number of pollution sources in the LA basin create ideal conditions for secondary organic aerosol (SOA) formation. A goal of this study is to identify as many individual components of the SOA as possible. This will provide much needed data to smog chamber experimenters and SOA formation modelers. The temporal and spatial aspects of this study will shed additional light on SOA formation mechanisms.

Experimental Matrix

Two sites: Urban (USC), and Receptor (UC Riverside)

One week (five days) at each sampling site for each season

Four time intervals each day: 7AM - 10:30AM, 11:00AM – 2:30PM, 3PM –6:30PM, and 7:00PM – 6:30AM

Weather conditions and traffic patterns should remain constant throughout each week, and preferably, throughout the entire study.

When: August, to maximize effect of photochemistry; and January, a low photochemical and cold weather sample

Progress

The first round of sampling has been completed. From August 12 to August 16, 2002, sampling was conducted on the rooftop of a 3-story building at the University of Southern California campus (urban site). From August 26 to August 30, 2002, sampling took place at the University of California, Riverside Citrus Research Center and Agricultural Experiment Station (CRC-AES) adjacent to an existing SCAQMD air sampling facility (receptor site).

Analysis for particle mass based on the MOUDI Teflon substrates are shown in the following two figures. PM2.5 mass peaked midday at USC and in the morning at Riverside. At both sites, Ultrafine PM mass was higher in the midday and evening than the morning or overnight. Ultrafine mass concentrations were significantly higher in Riverside than at USC.

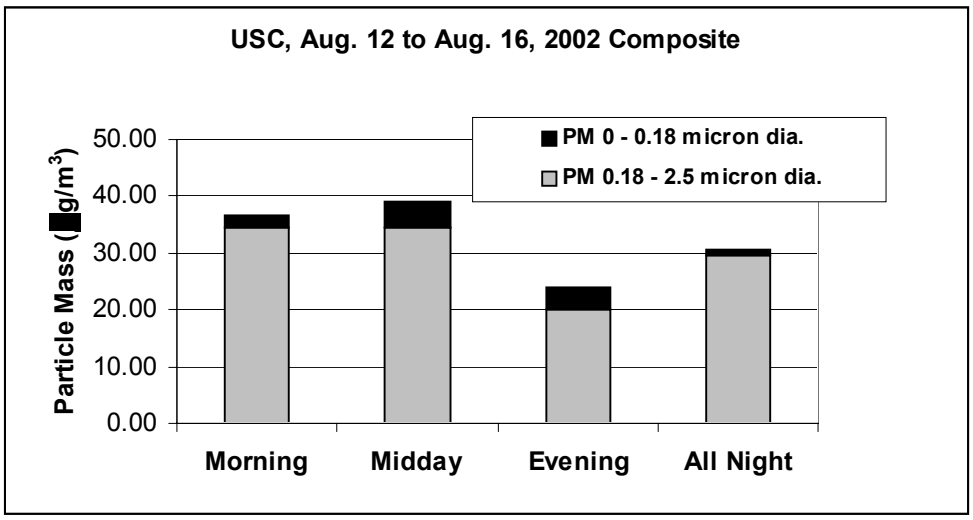

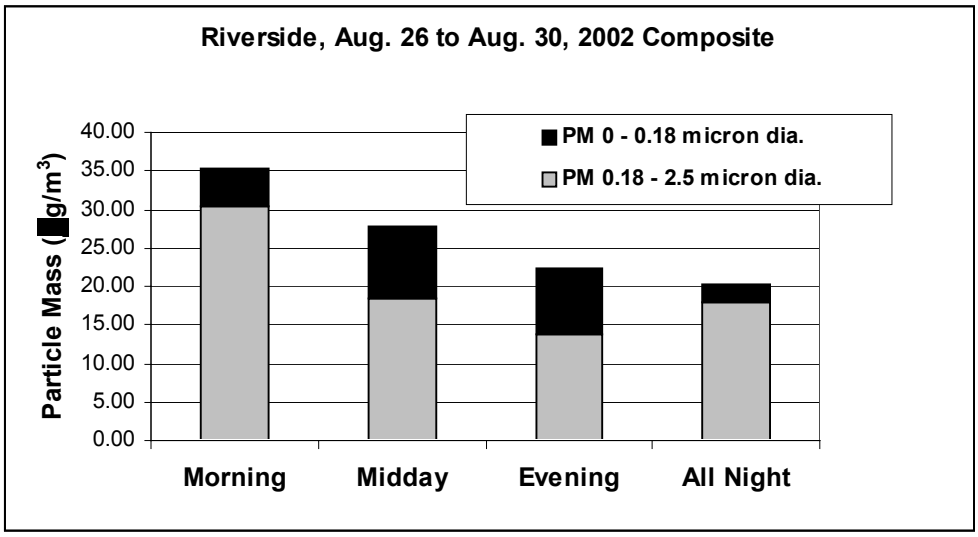

Organic carbon and elemental carbon analysis have just been completed for the summertime samples and are currently being evaluated. Organic speciation by GC/MS and ion chromatography are currently underway.

The wintertime tests are now scheduled for the weeks of January 13th (USC) and January 27th (Riverside), and preparations are currently underway.

8. Characterization of PAH and PAH-Derivatives

Background

The goal of this series of studies is to characterize the polycyclic aromatic hydrocarbons (PAHs) and PAH-derivatives present at sites chosen to represent source sites or downwind receptor sites and to investigate the atmospheric chemistry occurring at these sites during different seasons. Of particular interest are nitro-PAHs and nitro-polycyclic aromatic compounds (nitro-PACs) since these compounds are potent mutagens and have been observed as products of gas-phase atmospheric reactions of PAHs. During this reporting period ambient samples from Los Angeles [urban site at University of Southern California (USC)] and Riverside [approximately 50 miles downwind on a University of California Riverside (UCR) agricultural operations site] were analyzed for volatile PAHs and semi-volatile nitro-PAHs. Analyses of the filter samples for particle-adsorbed nitro-PAHs is on-going and will be reported in the next quarter.

Experimental section

Four time intervals per day were sampled during one week at Los Angeles (12-16 August 2002) and Riverside (26-30 August 2002). The daytime samples were 3.5 hours (morning 7 am-10:30 am, midday 11 am-2:30 pm and evening 3 pm-6:30 pm) and the nighttime sample was 11.5 hours (7 pm-6:30 pm).

The sampling sites were equipped with the following instrumentation: a Tenax solid adsorbent sampler, operating at 200 cm^3 min^{-1} for the daytime samples and at 100 cm^3 min^{-1} for the nighttime samples; a high-volume sampler with 2 polyurethane foam plugs (PUFs) located in series beneath a Teflon-impregnated glass fiber (TIGF) filter (20 cm × 25 cm) operated at ~0.6 m^3 min^{-1}. The analysis procedures were detailed in the September, 2002 quarterly report.

Each Tenax sample was spiked with deuterated internal standards and then thermally desorbed and analyzed individually by GC/MS. The values reported for the volatile PAHs for each time period are the average of the individual days. Prior to analysis by HPLC followed by GC/MS, the PUF extracts for each time period were pooled.

Results and Discussion

To date we have analyzed the Tenax samples for PAHs by GC/MS and the PUFs for semi-volatile nitro-PAHs using GC/MS with negative ion methane chemical ionization. The tables below give the concentrations of the volatile PAHs analyzed from the Tenax samples. Naphthalene has previously been reported as the most abundant PAH, being over an order of magnitude higher than the other targeted PAHs measured at the Children's Health Study sites (see, for example, the March-July progress report). As may be seen from the tables below, the alkyl-naphthalenes, especially 1- and 2-methylnaphthalene, will also be more abundant than the targeted PAHs. Because these alkylnaphthalenes are present in the gas-phase, their atmospheric lifetimes will be limited (estimated lifetimes due to hydroxyl radical reaction are a few hours) and products such as nitro-derivatives will be produced.

All 14 isomers of methylnitronaphthalenes (MNNs) and about 30 of the possible 55 isomers of the dimethylnitronaphthalenes (DMNNs) have been identified in HPLC fraction 4 of the ambient samples. To our knowledge, we are the first to report the presence of dimethylnitronaphthalenes in ambient atmospheres. Given in the table below are the ambient concentrations of the semi-volatile nitro-PAHs measured on the PUF samples (the filter samples are still being processed). Note that while the PAH concentrations are given in ng/m^3, the nitro-PAHs are reported in pg/m^3 units. Because standards of the methylnitronaphthalenes and dimethylnitronaphthalenes are not available, a response factor based on the response of the nitronaphthalenes and 2-methyl-1-nitronaphthalene (2M1NN) was used for all the MNN and DMNN isomers. It is interesting to note that while the ratio of naphthalene/MNs/DMNs is about 1: 0.5: 0.1-0.2 , the ratio of the sums of their nitro-derivatives, i.e., NNs/MNNs/DMNNs are more similar, presumably reflecting more reaction of the MNs and DMNs than of naphthalene.

USC Average Ambient Concentrations of PAHs for August 12-16, 2002

	0700-1030 hr	**1100-1430 hr**	**1500-1830 hr**	**1900-0630 hr**
	ng/m^3	ng/m^3	ng/m^3	ng/m^3
Naphthalene	**391.5**	**152.4**	**125.8**	**201.6**
2-MN	**168.4**	**48.0**	**48.7**	**84.0**
1-MN	**70.6**	**17.1**	**16.7**	**34.9**
Biphenyl	**8.3**	**3.5**	**2.4**	**2.1**
2-EN	**4.9**	**1.5**	**1.6**	**2.1**
1-EN	**1.6**	**0.6**	**0.5**	**0.5**
2,6/2,7-DMN	**9.2**	**1.8**	**2.0**	**4.4**
1,3/1,7-DMN	**9.4**	**1.6**	**1.8**	**4.1**
1,6-DMN	**5.0**	**1.0**	**1.2**	**2.6**
1,4-DMN	**1.4**		**0.3**	**0.6**
1,5/2,3-DMN	**2.4**	**0.5**	**0.6**	**1.2**
1,2-DMN	**2.0**	**0.7**	**0.5**	**0.7**

Key: MN = methylnaphthalene; EN = ethylnaphthalene; DMN = dimethylnaphthalene.

UCR Average Ambient Concentrations of PAHs for August 26-30, 2002

	0700-1030 hr	1100-1430 hr	1500-1830 hr	1900-0630 hr
	ng/m^3	ng/m^3	ng/m^3	ng/m^3
Naphthalene	**300.5**	**54.9**	**21.6**	**148.4**
2-MN	**113.2**	**12.4**	**6.4**	**50.5**
1-MN	**36.9**	**4.2**	**2.4**	**20.7**
Biphenyl	**6.1**	**3.6**	**2.7**	**2.3**
2-EN	**2.9**	**0.6**	**0.5**	**1.6**
1-EN				
2,6/2,7-DMN	**3.5**	**0.7**	**0.5**	**2.7**
17-DMN	**3.1**	**0.6**	**0.4**	**2.2**
1,6-DMN	**2.0**	**0.4**	**0.4**	**1.9**
1,4-DMN				
1,5/2,3-DMN	**0.9**			**0.7**
1,2-DMN	**0.7**	**0.8**		**0.4**

Key: MN = methylnaphthalene; EN = ethylnaphthalene; DMN = dimethylnaphthalene.

USC Average Ambient Concentrations of Nitro-PAHs for August 12-16, 2002

	0700-1030 hr	1100-1430 hr	1500-1830 hr	1900-0630 hr
	pg/m^3	pg/m^3	pg/m^3	pg/m^3
1-NN	**237**	**243**	**140**	**152**
2-NN	**258**	**243**	**112**	**99**
3-NBPh	**64**	**73**	**23**	**32**
2M1NN	**16**	**5**	**4**	**13**
1M8NN	**0**	**0**	**0**	**2**
2M8NN	**13**	**11**	**8**	**12**
2M4NN	**10**	**8**	**5**	**10**
1M2+2M5-NN	**16**	**14**	**9**	**14**
1M5NN	**72**	**93**	**50**	**47**
1M6+1M4-NN	**70**	**66**	**39**	**41**
2M7NN	**19**	**15**	**9**	**10**
2M6NN	**9**	**7**	**5**	**5**
1M7NN	**6**	**6**	**4**	**2**
1M3NN	**12**	**10**	**5**	**7**
SUM MNNs	**244**	**237**	**135**	**164**
SUM DMNNs	**167**	**127**	**75**	**133**

Key: NN= nitronaphthalene; NBPh = nitrobiphenyl; *x*M*y*NN = x-methyl-y-nitronaphthalene; DMNN = dimethylnitronaphthalenes (also includes ethylnitronaphthalenes).

UCR Average Ambient Concentrations of Nitro-PAHs for August 26-30, 2002

	0700-1030 hr pg/m^3	1100-1430 hr pg/m^3	1500-1830 hr pg/m^3	1900-0630 hr pg/m^3
1-NN	**190**	**201**	**142**	**354**
2-NN	**308**	**273**	**140**	**237**
3-NBPh	**103**	**84**	**82**	**40**
2M1NN	**8**	**3**	**67**	**31**
1M8NN	**0**	**0**	**2**	**7**
2M8NN	**13**	**7**	**19**	**22**
2M4NN	**15**	**5**	**9**	**34**
1M2+2M5-NN	**14**	**9**	**20**	**26**
1M5NN	**56**	**59**	**38**	**72**
1M6+1M4-NN	**64**	**48**	**36**	**55**
2M7NN	**23**	**14**	**7**	**14**
2M6NN	**12**	**7**	**7**	**8**
1M7NN	**8**	**7**	**3**	**3**
1M3NN	**13**	**9**	**8**	**11**
SUM MNNs	**227**	**167**	**214**	**283**
SUM DMNNs	**124**	**73**	**46**	**178**

Key: NN= nitronaphthalene; NBPh = nitrobiphenyl; *x*M*y*NN = x-methyl-y-nitronaphthalene; DMNN = dimethylnitronaphthalenes (also includes ethylnitronaphthalenes).

As may be seen from the Figure 1 below, the PAHs were highest during the 0700-10:30 time period at UCS (August 12-16, 2002), presumably reflecting the input of morning traffic. The decrease in concentrations during 1100-1430 is the result of an increasing inversion height and atmospheric reactions. Note that the MNs and DMNs, which are more reactive than either naphthalene or biphenyl toward hydroxyl (OH) radical reaction, show larger percent decreases from the morning sample. The PAH concentrations measured at UCR during August 26-30, 2002 were always lower than those of the corresponding time periods measured at UCS.

In contrast to the PAH concentrations, the nitro-PAHs were often more abundant in Riverside (see Figure 2), consistent with atmospheric formation being the major source of these nitro-PAHs. 3-Nitrobiphenyl, whose only known source is the atmospheric OH radical-initiated reaction of biphenyl, is consistently higher during the daytime than during the nighttime at both sites, and at USC the highest 3NBPh/Biphenyl ratio occurs between 1100-1400 when the OH

radical concentration is expected to be at its maximum (see Figure 3). At UCR the ratios of the nitronaphthalenes to naphthalene and the methylnitronaphthalenes to the methylnaphthalenes steadily increase during the daytime, suggesting transport of an aged, reacted air mass into Riverside.

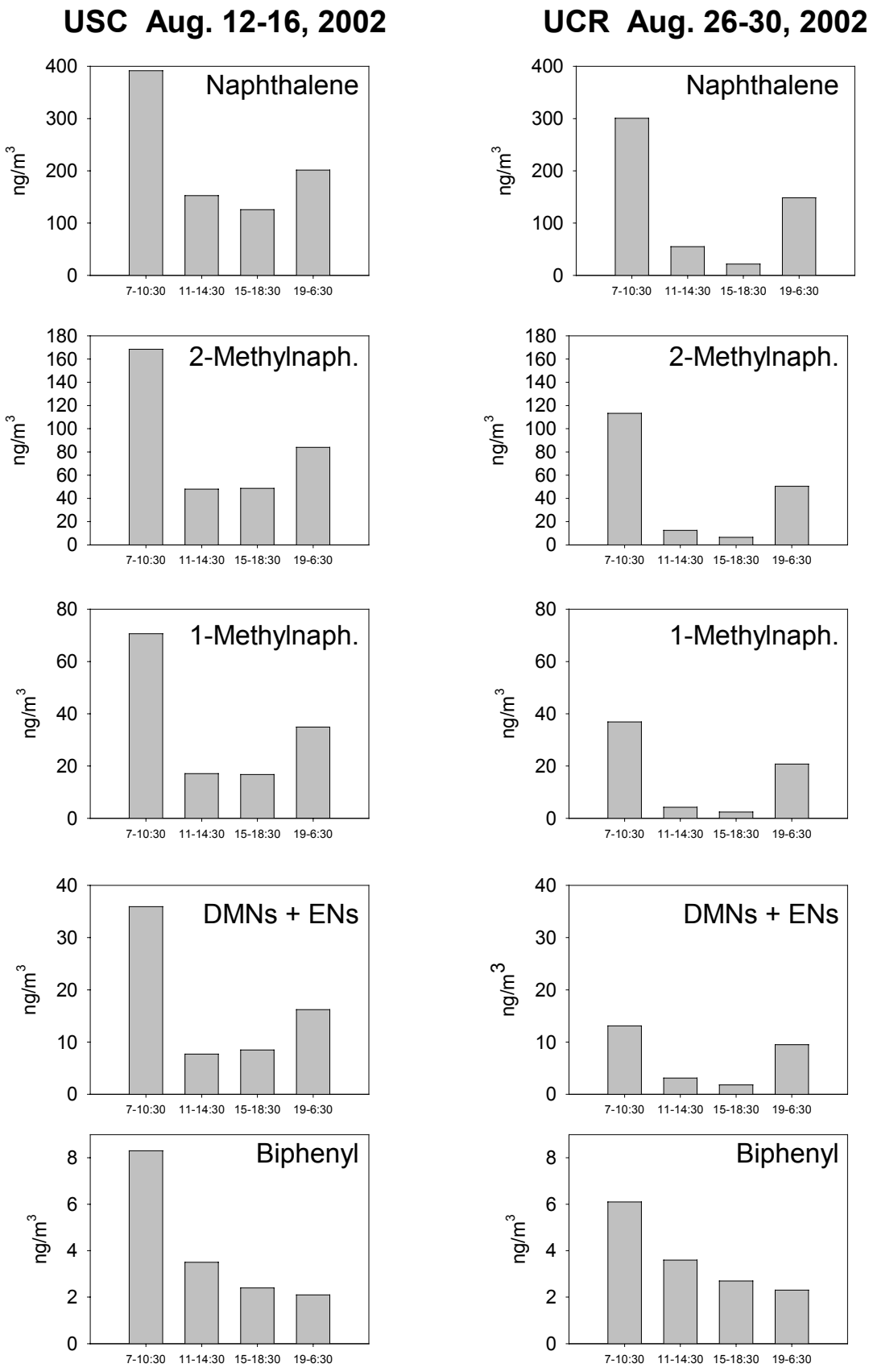
USC Aug. 12-16, 2002
UCR Aug. 26-30, 2002
Naphthalene
2-Methylnaph.
1-Methylnaph.
DMNs + ENs
Biphenyl
ng/m3
7-10:30
11-14:30
15-18:30
19-6:30

Figure 1

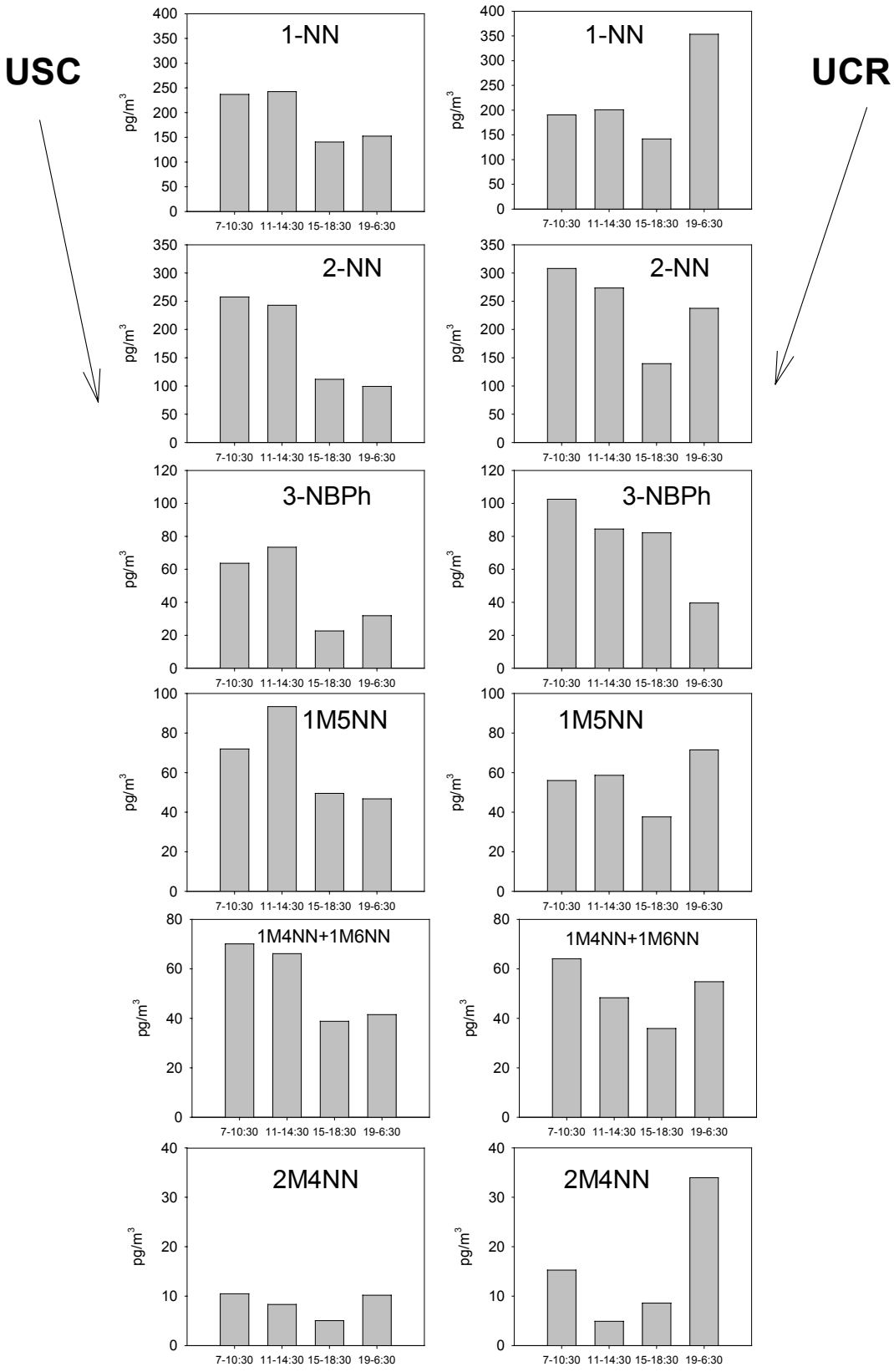
USC
UCR
1-NN
2-NN
3-NBPh
1M5NN
1M4NN+1M6NN
2M4NN
pg/m3
7-10:30
11-14:30
15-18:30
19-6:30

Figure 2

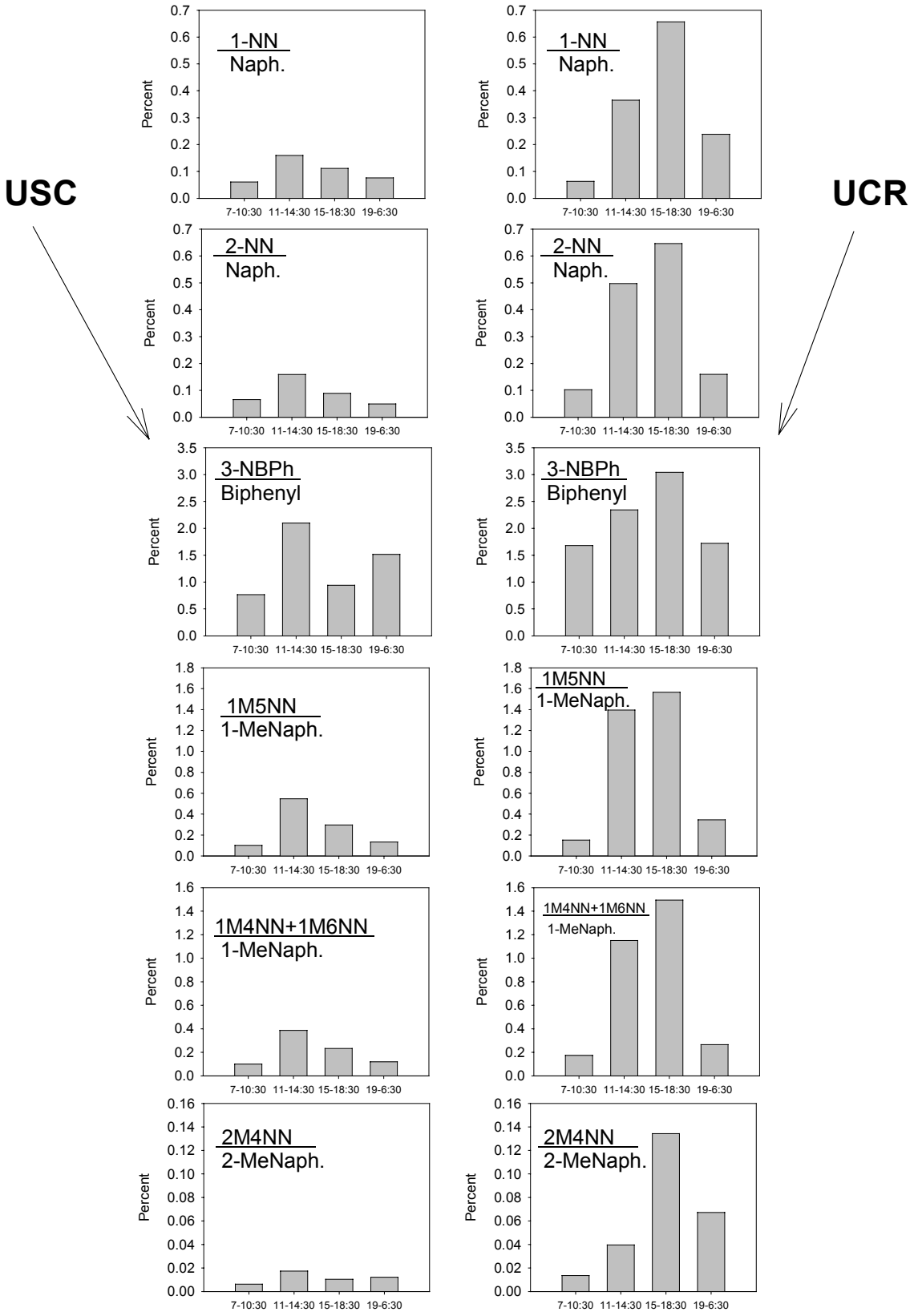
USC
UCR
1-NN
Naph.
2-NN
Naph.
3-NBPh
Biphenyl
1M5NN
1-MeNaph.
1M4NN+1M6NN
1-MeNaph.
2M4NN
2-MeNaph.
Percent
7-10:30
11-14:30
15-18:30
19-6:30

Figure 3

The highest concentrations of 1-NN and 2M4NN occur at Riverside during the nighttime. Comparisons, based on laboratory chamber studies, of the profiles of the *x*M*y*NN isomers formed from the OH radical-initiated reaction of 1- and 2-methylnaphthalene with the profile from the NO_3 radical-initiated reaction of the MNs, have shown 2-methyl-4-nitronaphthalene and 2-methyl-1-nitronaphthalene to be enhanced relative to the other MNN isomers in the NO_3 reactions. The maximum in the concentrations of 2M4NN and 2M1NN (see table) at UCR in the 1500-1830 and nighttime samples suggests the occurrence of NO_3 chemistry in the air mass reaching Riverside in late afternoon or early evening. This is consistent with the highest 1-NN concentration in the nighttime sample and the highest ratio of 1-NN/naphthalene in the 1500-18:30 samples because 1-NN is formed in greater abundance than 2-NN from the NO_3 radical-initiated reaction of naphthalene.

As noted, dimethylnitronaphthalenes were also observed at both the USC and UCR sites. Work is underway to try to identify dimethylnitronaphthalene isomers and their formation pathways. Preliminary results show that both OH and NO_3 radical-initiated reactions of dimethylnaphthalenes will result in nitro-DMN formation.

Future plans

Winter sampling is planned for Los Angeles (at USC) on January 13-17, 2003 and at Riverside (agricultural operations site at UCR) on January 27-31, 2003. Again Tenax samples for volatile PAHs, PUF plug samples for semi-volatile PAHs and nitro-PAHs and filter samples for particle-adsorbed PAHs and nitro-PAHs will be collected. It will be interesting to find out whether lower nitro-PAH levels will occur, reflecting less atmospheric formation.

9. Continuous Coarse and Fine PM Measurement

Introduction

During this quarter, a Continuous Coarse Monitor (CCM) was set up in the Supersite trailer and began operation on 11/01/02. Data will be generated at USC until the trailer moves to the next site. At that point the instrument will be evaluated for continuation of sampling. Co-located with the CCM are a Scanning Mobility Particle Sizer-Aerodynamic Particle Sizer (SMPS-APS) tandem, an ESP differential Tapered Element Oscillating Microbalance (TEOM), and a PM2.5 Beta Attenuation Monitor (BAM). Both coarse and fine PM mass concentrations have been tracked each half hour. Data are downloaded about every two weeks from the CCM, SMPS-APS, and BAM. Rupprecht and Patashnick Co., Inc. download the ESP TEOM data periodically and share it with us as it is available.

Results

The coarse PM data for the last week in November and the first week in December are presented in Figures 1 and 2. As evidenced from the figures, the CCM and APS track each other fairly well with occasional disagreement, which is most likely due to incorrect assumptions by the APS about the density of the PM. The stability of the PM concentrations clearly affects how well the instruments agree with each other. When mass concentrations are highly variable, the instruments have more separation. This is expected because each instrument responds to rapid changes in concentration with different reaction and recovery times. The missing CCM data on December 3rd is due to instrument maintenance. The PM2.5 data is not shown here because the SMPS was down for this period, and the ESP TEOM data is not yet available.

Figure 1: Coarse Vs. Fine 11/25-12/1 2002

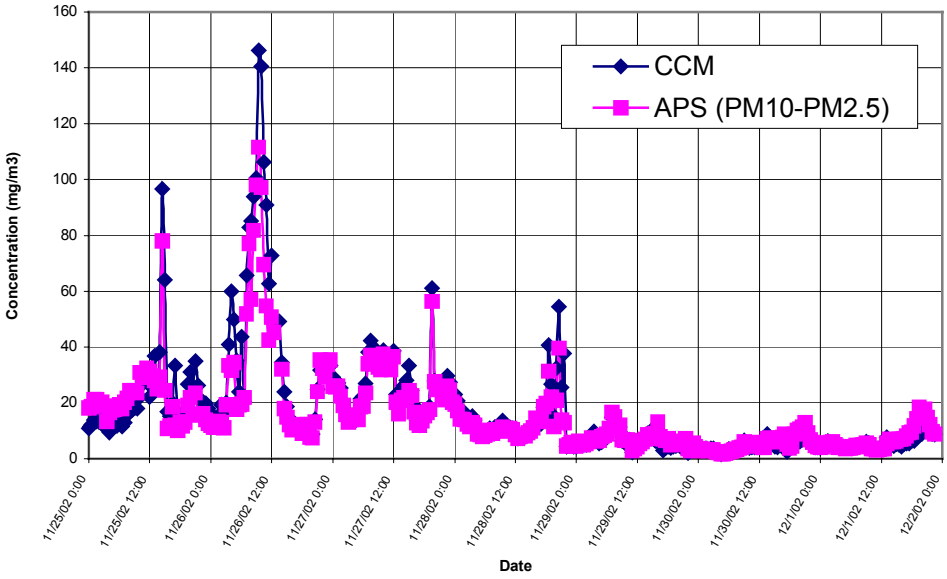

Figure 2: Coarse Vs. Fine 12/2-12/9 2002

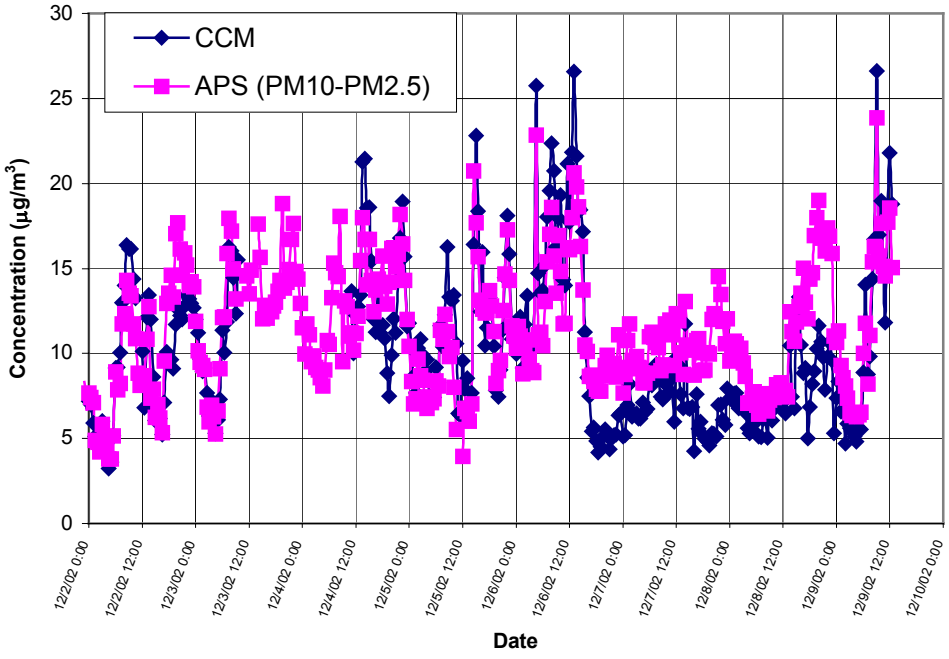

Problems

Due to a faulty flow controller, the CCM's TEOM sometimes experiences flow fluctuations. A new flow controller will be switched with the old one before the beginning of the

next quarter. The SMPS experienced some maintenance downtime for a period of two weeks in late November. A power outlet malfunction created a time error for the SMPS-APS data files. The errors were corrected on the data sheets and the outlet was fixed.

Next Quarter

Coarse and fine PM will continue to be monitored and all data should be available for the next quarterly report. At that time, the analysis will include the effect of wind speed and direction on the mass concentrations of both size modes. The continuous data will also be averaged over 2-hour intervals in order to correlate it to the BAM PM2.5 measurements. Reliable PM2.5 data is expected from the ESP TEOM by the end of next quarter, and it will be added to the above figures to display times during which the modes track and times during which they diverge. Finally, when enough data is available, representative weeks will be averaged according to hour of the day in order to investigate diurnal variation of both size modes.

10. Continuous PM 2.5 Mass by the Differential TEOM® MONITOR and a Continuous Size Segregated Nitrate Monitor in Claremont California: Evaluation of the Dynamics of Nitrate Volatilization

As part of the Los Angeles based U.S. EPA sponsored Southern California Particle Center and Supersite (SCPCS), semi-continuous (10-minute) particulate matter less than 2.5 micrometers (PM2.5), and semi-continuous (10-minute) size segregated particulate nitrate (2.5-1.0 μm, 1.0-0.5 μm, & 0.5~0.1 μm) were measured using the Differential TEOM® monitor (Patashnick, et al., 2000; Jaques, et al., 2002; October 2002 Los Angeles Supersite quarterly report), and a cascaded Integrated Collection and Vaporization Cells (ICVC) (Stolzenburg, et al., 2002; Fine, et al., 2002), respectively. The Differential TEOM monitor employs an electrostatic precipitator to resolve artifactual changes in filter mass change related to semi-volatile PM. The electrostatic precipitator (ESP) is activated in alternating 5-min periods to remove particles from the sample air stream. The mass change of the filter with the ESP activated is subtracted from the mass change during the normal collection (with the ESP off) to provide an artifact-corrected mass.

The results presented are part of a poster that we plan to present at the Particulate Matter: Atmospheric Sciences, Exposure and the Fourth Colloquium on PM and Human Health in Pittsburgh (March 31-April 4, 2003), and submit to the meeting's special issue proceedings. The full data to be presented will be from both the Claremont and USC Supersites. Herein, we compare the mass lost during the "ESP-on" cycle to ambient particulate nitrate concentrations measured by the ICVC. Figure 1 presents lab results using the Differential TEOM to measure polydisperse NH4NO3 onto a new filter. Aerosol was sampled for about 8 hours, followed by filtered air. The hourly average PM2.5 mass data is the difference between the ESP off and on cycles. The off cycle represents activity without PM collection, when the kinetics of volatilization can be observed. Once filter loading develops, during the first couple hours, volatilization can be seen by observing the ESP-on trend increase in negative mass, and then

once the PM filter mass has stabilized, the negative ESP-on mass becomes lower. Once aerosol free air is sampled the ESP-on mass asymptotes to zero over a 9 hour period.

For measurements at Claremont, episodes of PM2.5 are often highly associated with ammonium nitrate, and they generally correspond with high daytime temperatures, peaking during mid-afternoons. Figure 2 presents continuous ambient Differential TEOM and NH4NO3 data for a 3 day period in February and a 2 day period at Claremont, both during NO3 episodes. The peak PM2.5 mass and NH4NO3 coincides with daytime high temperatures. Figures 3 presents a scatter plot of the 10 minute February data (Figure 2a) of the ESP-on mass versus the NH4NO3. The negative slope of -0.46 and high correlation of 0.75, clearly show that desorption occurs from the filter with ambient NH4NO3 collection. If should be noted, though, that the 5-minute ESP-on and –off cycling protocol subtracts out these artifact effects (Jaques, et al., 2002). Time delayed TEOM data (maximized at 40 minutes) vs real time NH4NO3 also suggests delayed volatilization effects. Close examination of the data suggests that the rate of volatilization is non-linear, especially following high periods of PM2.5 ammonium nitrate. It also appears that the volatilization of nitrate occurs more rapidly when freshly loaded onto the filter.

References:

Jaques PA, Ambs JA, Grant WL, Sioutas C. Field Evaluation Of The Differential TEOM® Monitor For Continuous $PM_{2.5}$ Mass Concentrations. Submitted For Publication to *Aerosol Sci. and Technol*, October 2002.

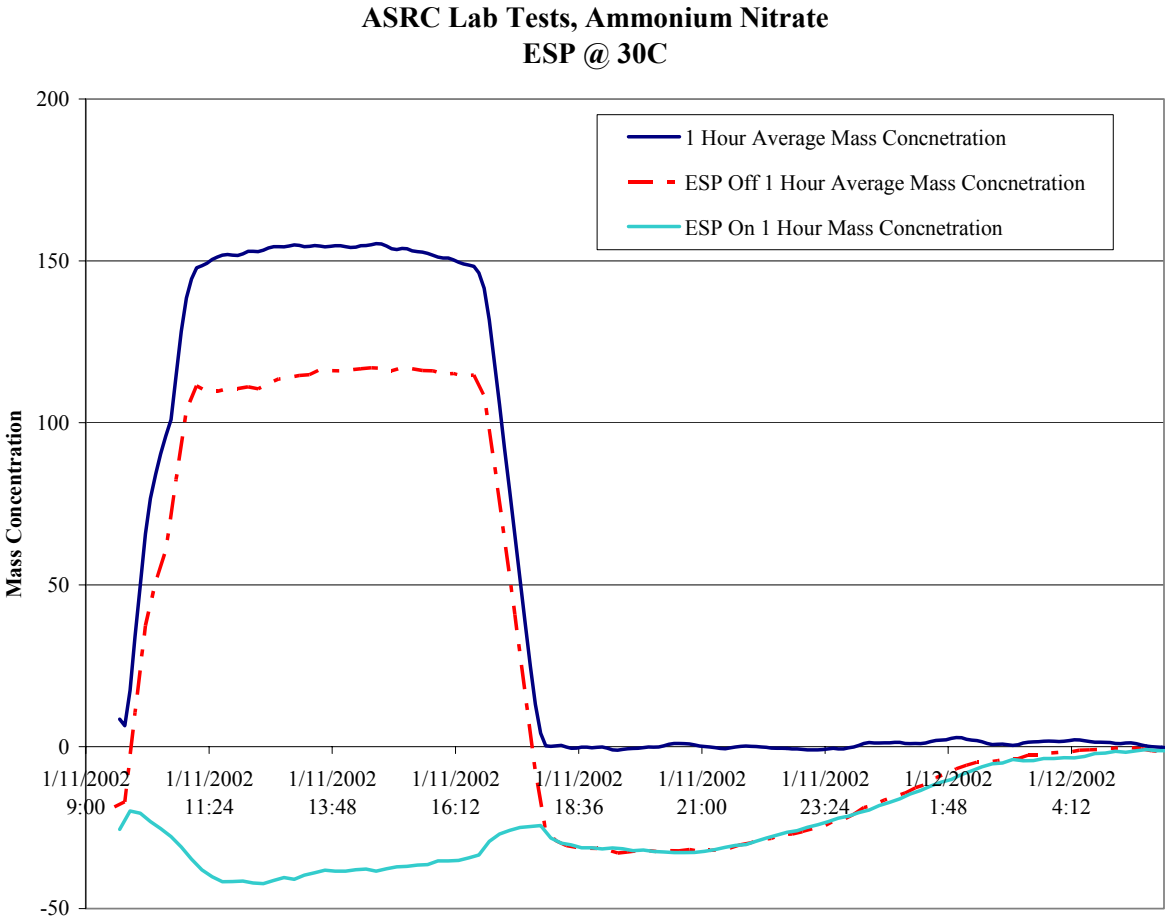

Figure 1. Laboratory tests of Differential TEOM, evaluating the kinetics of Ammonium Nitrate volatilized from the filter.

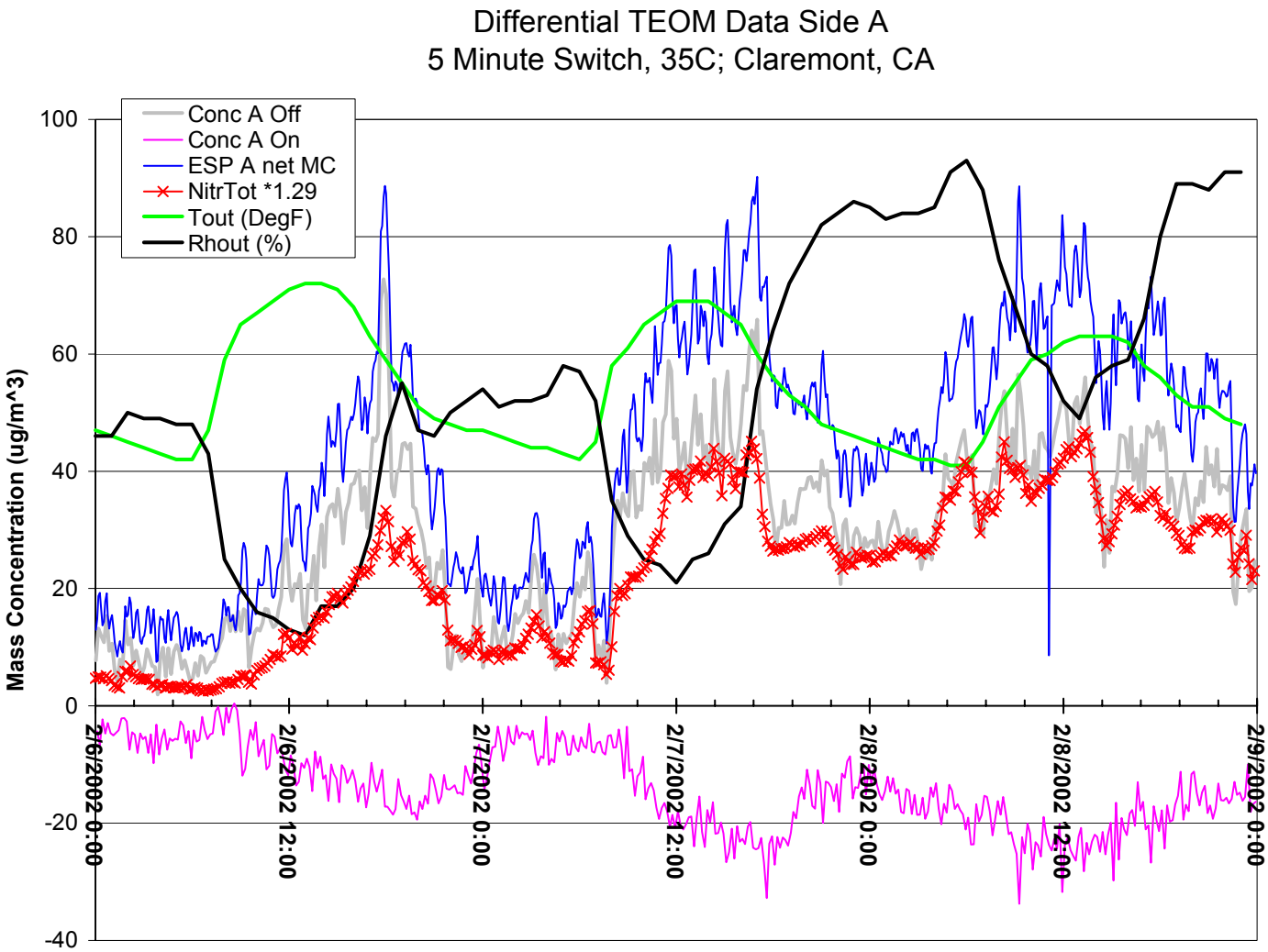

Figure 2a. Selected 5 minute Differential TEOM mass data with the ESP on and off, compared with 10 minute PM2.5 Ammonium Nitrate measured by the ADI system for a 3 day period during February 2002 – with Temp and RH data.

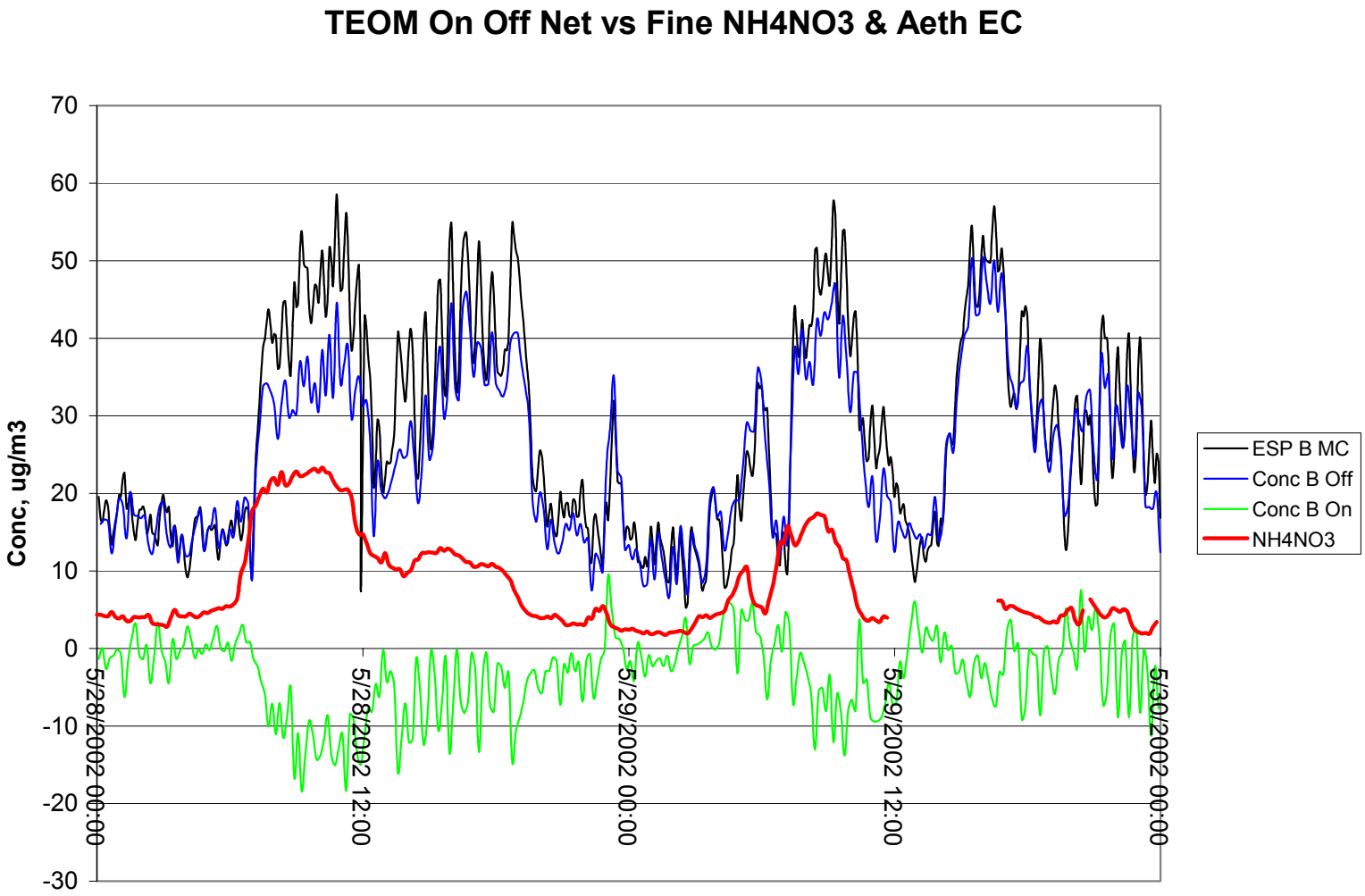

Figure 2b. Selected 5 minute Differential TEOM mass data with the ESP on and off, compared with 10 minute PM2.5 Ammonium Nitrate measured by the ADI system for a 2 day period during May 2002.

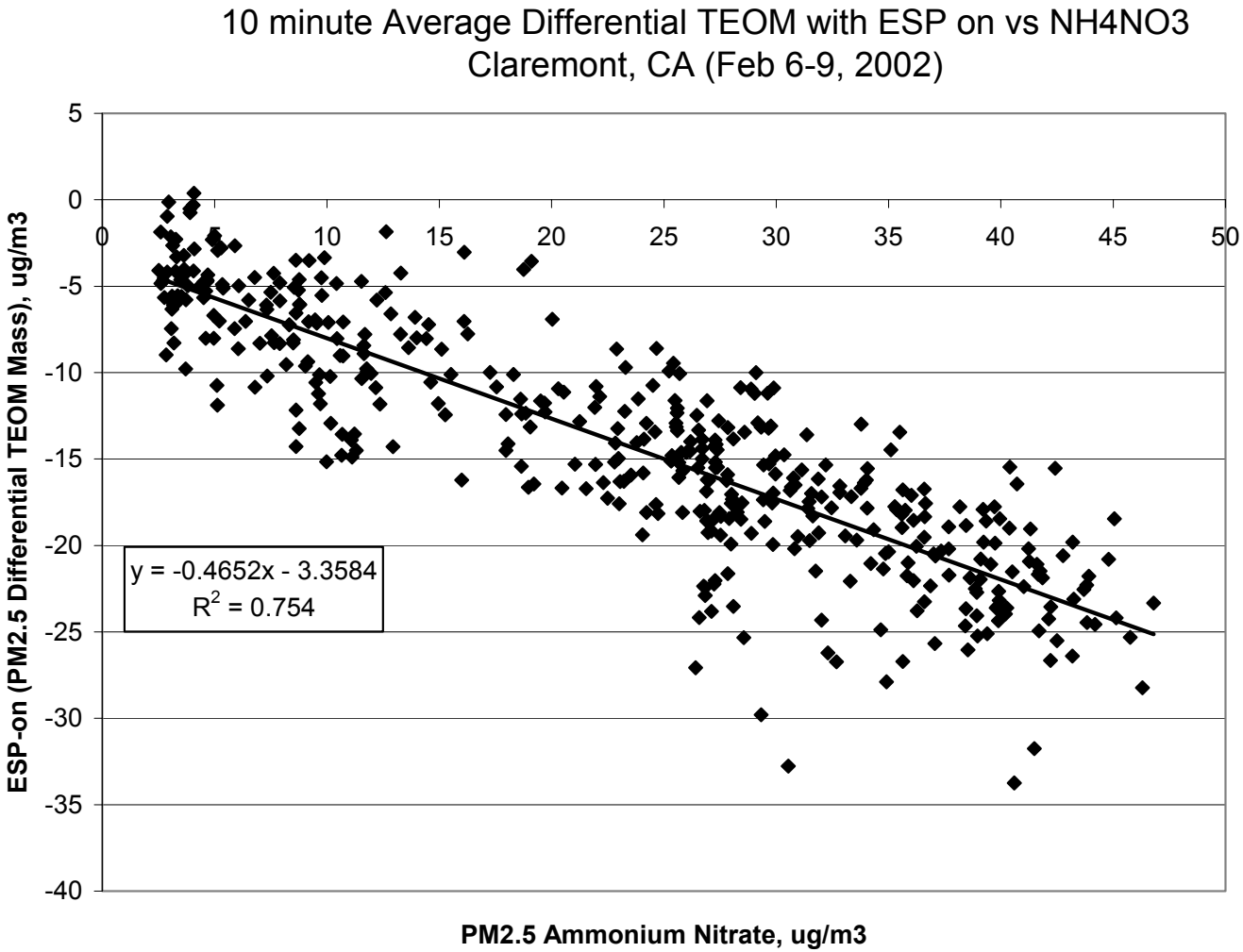

Figure 3. Scatter plot of 10-minute averaged Differential TEOM data with the ESP on versus that of NH4NO3 for February 6-9, 2002 at Claremont, CA.

11. Chemical Characterization of Ultrafine Particles in the LA Basin

The plan for this study is to conduct bi-weekly MOUDI/Nano-MOUDI sampling in the following sites:

Date	USC	Long Beach	Riverside	Upland
Fall	**Oct. 2-Oct. 15**	**Oct. 16-Oct. 29**	**Oct. 30-Nov.12**	**Nov. 13-Nov. 26**
Winter	**Jan. 14-Jan. 27**	**Jan. 28-Feb. 10**	**Feb. 11-Feb. 24**	**Feb. 25-Mar. 10**
Spring	**Apr.1-Apr.14**	**Apr.15-Apr.28**	**Apr. 29-May 12**	**May 13-May 26**
Summer	**July 15-July 28**	**July 29-Aug.11**	**Aug.12-Aug.25**	**Aug.26-Sept.8**

The following stages of the MOUDI and Nano-MOUDI are employed (nm):
2500-1000
1000-320
320-180
180-100
100-56
56-32
32-18
18-10

All substrates will be 47 mm pre-baked aluminum.

The following analyses will be performed:

- Gravimetric
- EC/OC
- PAH
- Quinone
- IC

Introduction

Aluminum substrates were pre-baked and sealed prior to October 1. Six substrates per two-week period were used. The MOUDI/Nano-MOUDI combination was employed at each site listed above from October 2-November 26, 2002 (highlighted in sampling schedule). Sampling was non-stop for the listed periods with no change of substrates except between sites. Upon completion of each site, the substrates were split into two pieces. Three-fourths were sent to Dr. Tony Miguel at UCLA for organics analyses, and one-fourth was sent to Rancho Los Amigos for ion chromatography. The chemical analyses have been ordered, but no results have yet been received.

Results

The following figures show the mass concentrations as a function of particle size collected. Figures 1-4 represent data obtained from USC, Long Beach, Riverside, and Upland, respectively. USC displays the highest ultrafine PM mass concentrations, followed by Long Beach. Riverside and Upland have the lowest ultrafine levels and are very close in magnitude to one another. These results are expected because USC and Long Beach are both source sites, impacted directly by vehicular emissions which are characterized by an appreciable fraction of PM in the ultrafine mode as a result of a freshly emitted aerosol. Riverside and Upland are receptor sites in which PM are either produced by secondary reactions or arrive after long-range transport from source sites. During this time of this particular year, photochemistry contributed very little to ultrafine particle production because of abnormally cool and cloudy weather. Thus, receptor sites had very low ultrafine particle concentrations. Organic and elemental carbon data is still pending, and ion chromatography data has just been partially received. These will all be included in the next report.

Problems

Some of the measurable masses on the aluminum substrates in the 10-32 nm range are at or close to the detection limits.

Next Quarter

The next phase of sampling will occur in what is the winter season in the LA basin. The same four sites will be visited from January to March.

Figure 1: USC Fall Ultrafine PM

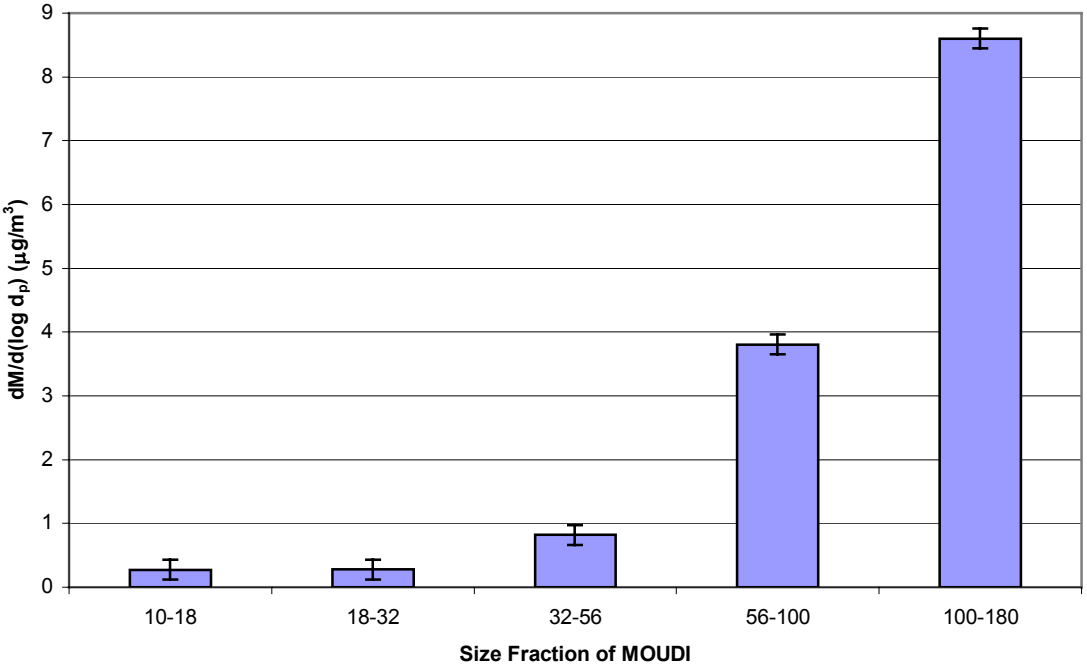

Figure 2: Long Beach Fall Ultrafine PM

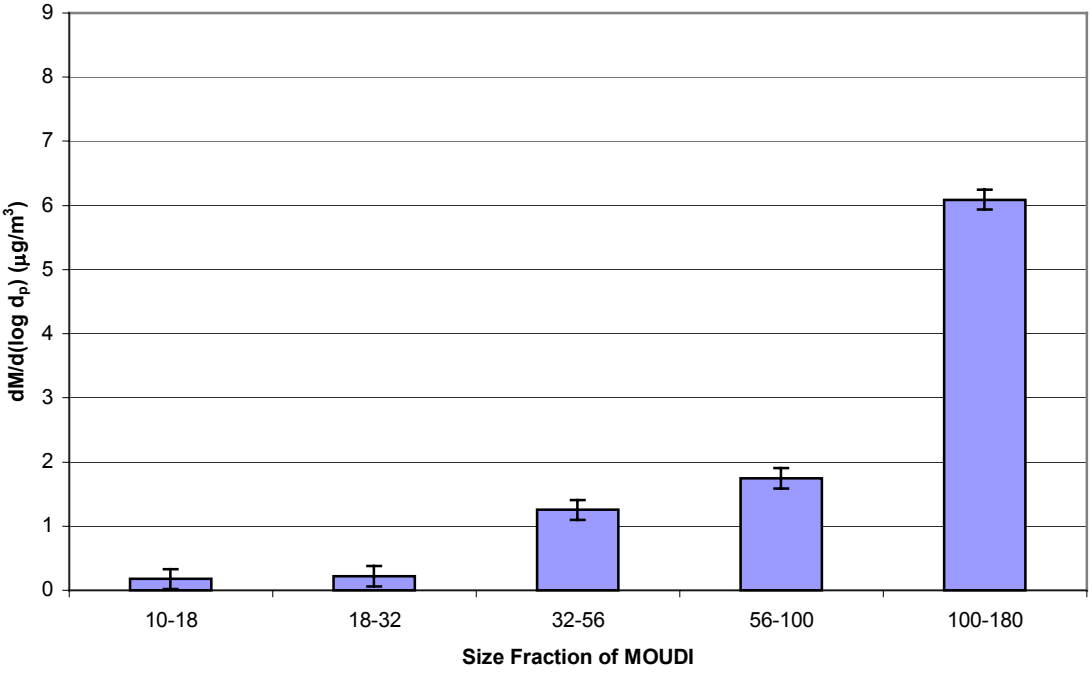

Figure 3: Riverside Fall Ultrafine PM

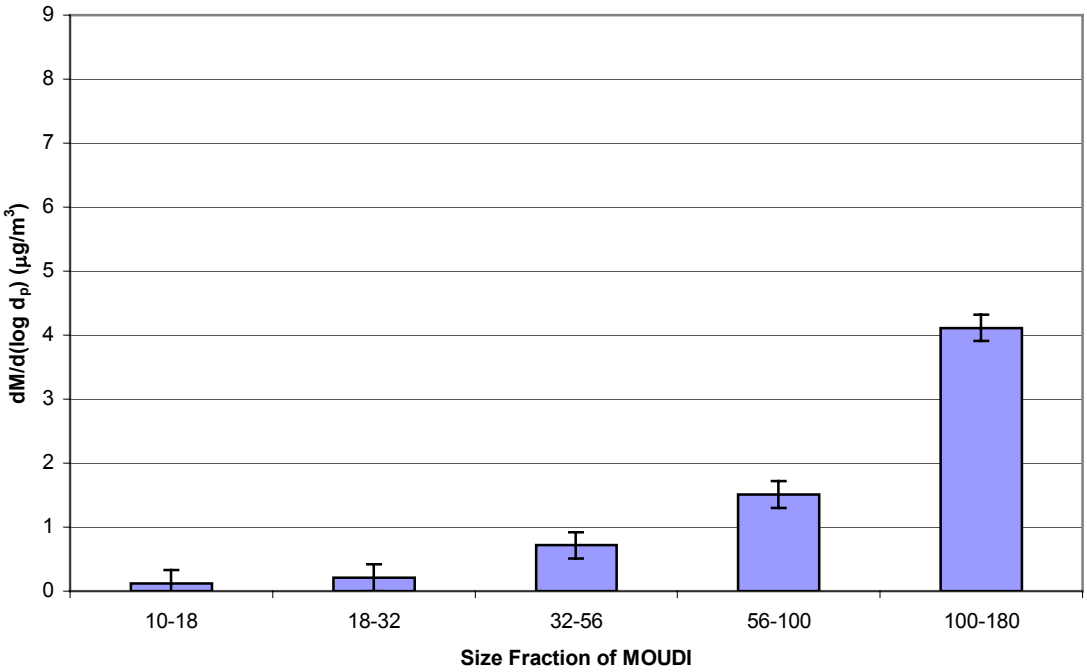

Figure 4: Upland Fall Ultrafine PM

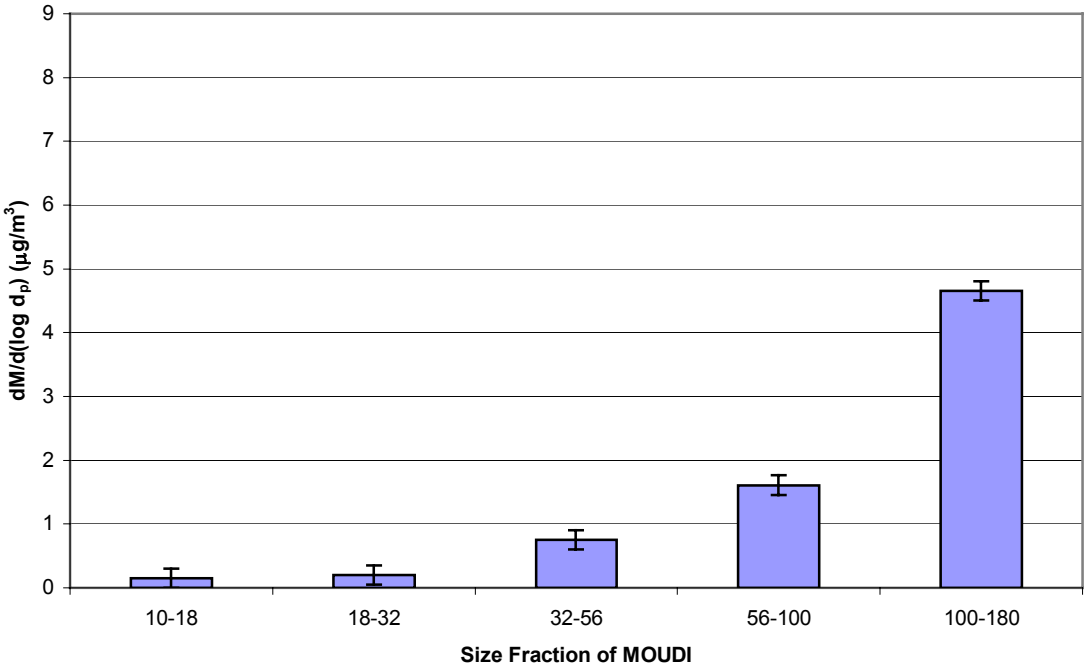

12. Automated, Size- and Time-Resolved Measurements of Particulate Carbon and Nitrate

From September to December 2002, we have simultaneous, size-resolved data on $PM_{2.5}$ nitrate and carbon concentrations at the USC sampling site. Measurements are made for both species using our cascaded integrated collection and vaporization systems (ICVS) as described in previous reports. Both ICVS's were shut down at the Claremont site on 9/12/02. Data collection at the USC site began on 9/25/02 and will continue into 2003.

The humidity control system from the Carbon ICVS was removed for laboratory testing to improve humidity stability in September. The controller was reconfigured in our lab and returned to the Carbon ICVS during installation at the USC site. The existing Nitrate ICVS humidity controller was reconfigured in a similar manner on-site. Overall noise in the RH control for both systems was reduced. Occurrences of large deviations from the 65% RH set point were also reduced. There were two distinct two-day periods (11/19/02-11/21/02 and 11/25/02-11/27/02) when the controlled RH on both systems hovered near 45%. It is unclear why this occurred, though it may simply be due to exceptionally low ambient humidity during those periods.

The Nitrate ICVS shows more variability in the controlled RH than the Carbon ICVS. As stated in previous reports, the Carbon ICVS controlled humidity water bubbler was moved inside the ventilated instrument enclosure to ensure it remained near ambient temperature. This modification has yet to be made on the Nitrate ICVS, and its bottle remains external and is subject to the trailer temperature.

The switch box that allows both computers to be displayed through one monitor malfunctioned, causing delays in restarting the Nitrate ICVS. The new switch box was installed on 11/19/02 and has corrected the problem.

Seven days of recent raw data are included below. In Figure 1 the diurnal variation in nitrate concentration can be seen. During the period shown, maxima occur between 10:00 and 11:00 and are driven mainly by the droplet mode of 0.5-1.0 μm, though the coarse mode of 1.0-2.5 μm follows the same general trends.

Carbon ICVS data shown in Figure 2 is more noise than the Nitrate ICVS data. However, a marked absence of mass on Cell B (0.5-1.0 μm) is noted. The concentrations detected on Cell A (1.0-2.5 μm) and Cell C (0.1-0.5 μm) are roughly equal, demonstrating a very large number of fine carbonaceous particles, enough to produce a mass comparable to the that of the coarse particles.

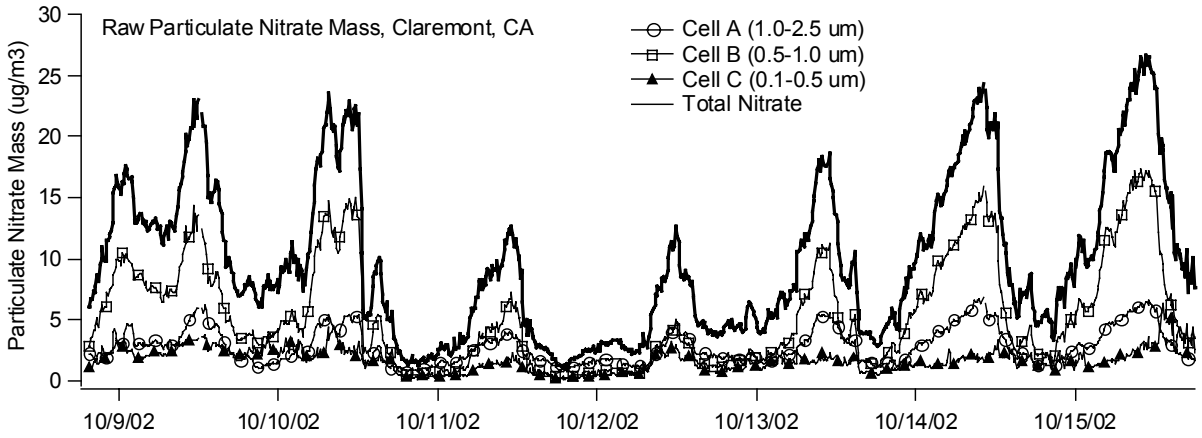

Figure 1. Particulate carbon mass by size fraction, USC site, California.

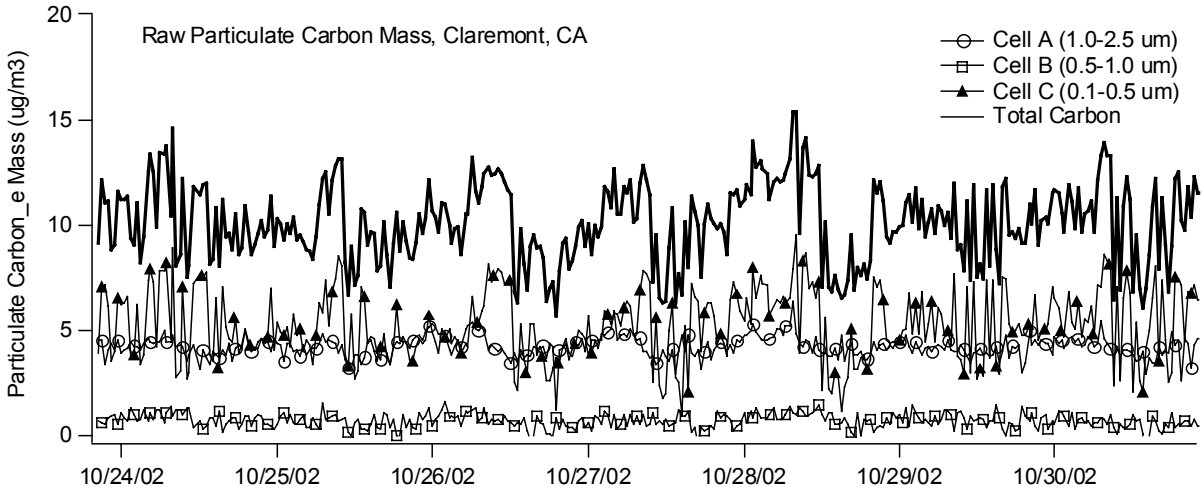

Figure 2. Particulate nitrate mass by size fraction, USC site, California.

13. Particle Size Distribution of Polycyclic Aromatic Hydrocarbons, Elemental and Organic Carbon, Sulfate and Nitrate Measured in Claremont: Part II

Summary

This report (Part II) describes the remaining size distribution measurements of polycyclic aromatic hydrocarbons (PAH), EC, OC (June and July 2002), and of sulfate and nitrate for the full 10-month period in Claremont, completing four seasons of measurements. 24-hr samples were collected once every week, from midnight to midnight, using MOUDI impactors with four or five stages as described in Part I. The samples were composited into monthly periods into three aerodynamic diameter size intervals: 0-0.18 μm (ultrafine mode I), 0.18-2.5 μm (accumulation mode II), and 2.5-10 μm (coarse mode III). PAH were separated and quantified by gradient HPLC with selective fluorescence detection; EC and OC were measured using a thermo-evolution/optical transmission carbon analyzer, nitrate and sulfate by ion chromatography. The effects of average ambient temperature and RH on species concentration measurements are discussed.

EXPERIMENTAL SECTION

Details of sample collection and chemical analysis are described in the previous (Part I) report.

RESULTS AND DISCUSSION

Normalized PAH Size Distributions:

The target PAH studied were grouped according to their sub-cooled vapor pressure, p^o_L. The group of more volatile PAH ($\log[p^o_L]$ from -0.95 to -2.06) includes PHE, ANT, PYR, and FLT. The group of less volatile PAH ($\log[p^o_L]$ from -3.22 to -7.04) includes BAA, CRY, BGP, BAP, BBF, BKF, DBA and IND. Their names, MW, and individual sub-cooled liquid vapor pressures are described in Part I. The normalized PAH size distributions (by group) and total PAH mass (C) measured in June and July, 2002 are shown in Figure 1. As discussed in Part I, for each monthly composite, the distributions are similar for both PAH groups. However, the distribution shapes varied quite markedly over the observed period. Whereas from October, 2001, to January,

2002, the distributions contained no coarse modes, from February on, the distributions showed a prominent coarse mode, for both PAH groups. The increase observed in the coarse mode PAH during this period may have resulted from coagulation with coarse mode nitrate particles (see Figures 3-A and 3-B).

Normalized EC and OC Size Distribution:

Normalized EC and OC size distributions and total mass (M) measured in Claremont in June and July 2002 are shown in Figure 2. As observed in previous months, the EC and OC distributions are distinguished by prominent modes in the ultrafine and accumulation size mode, and smaller coarse modes. The largest fraction of EC mass is in the ultrafine mode; typical of combustion emissions, also seen for OC. However, the largest fraction of the OC mass is found in the accumulation mode.

Normalized SO_4^{-2} and NO_3^- Size Distribution: Normalized SO_4^{-2} and NO_3^- size distributions and total mass (C) measured in Claremont from October 2001 to July 2002 are shown in Figures 3-A and 3-B. This information is new in this report. The size distributions of sulfate are similar throughout the 10-month period, with major modes in the accumulation and coarse modes, as observed previously in the LA basin. Coarse mode sulfate is associated with primary sea salt particles, while the smaller mode results from gas-to-particle conversion processes. Contrasting this observation, the distribution of nitrate varied gradually during the entire period. While the fraction of nitrate mass found in the coarse mode was about equal or somewhat smaller than the accumulation mode in previous months, beginning in March 2002, the fraction of nitrate mass in the coarse mode increased monotonically, becoming the major mode in July! While particulate nitrate collection is known to be prone to sampling artifacts, the observed increase in the coarse mode nitrate suggest that it may result from reactions of sea salt with photochemically produced HNO_3, as both the temperature and RH rise towards the summer (See Fig. 8) with ensuing increasing water condensation.

Trends and Correlations of Mean Ambient Temperatures with PAH, EC and OC Total Mass:

Figures 4 and 5 show, respectively, the seasonal trends of measured average monthly total mass of PAH and EC-OC --along with temperature. For total species mass, the Pearson correlation coefficients (r) were high for EC (0.78), OC (0.77), BAA-IND (-0.60), and PHE-ANT groups (0.53). The correlations for the individual modes were discussed in detail in Part I.

Trends and Correlations of Mean Ambient Temperatures with Sulfate and Nitrate Total Mass:

The seasonal trends of measured average monthly total mass of SO_4^{-2} and NO_3^- --along with temperature are shown in Figure 6 and 7. For total species mass, the Pearson correlation coefficients (r) were high for SO_4^{-2} (0.77), but insignificant for NO_3^- (0.02). As Figure 7 shows, temperature, and sulfate and EC concentrations track each other very well during the entire period. Average monthly temperature and %RH seasonal trends for the period are shown in Figure 8.

Conclusions

The following conclusions and basic hypothesis may be drawn from the observations reported in Parts I and II of this Report:

- **PHE-ANT:** High positive correlation with the more volatile group suggests increased contribution from diesels, and partitioning from the vapor-phase during transport across the LA basin.
- **BAA-IND:** Negative correlations of temperature with the less volatile PAH in modes I and II suggest desorption from the particle-phase (when the temperature increases) and partitioning from the vapor to the particle-phase (when the temperature decreases). Positive correlations with the coarse mode suggest coagulation of these PAH with coarse particles such as nitrate resulting from reactions of photochemically produced HNO_3 with sea salt as both the temperature and RH rise towards the summer.
- **EC:** High positive correlation of temperature with EC suggests increased transport of diesel emissions from the central LA Basin to Claremont as the temperature increases towards the summer.

- **OC:** High positive correlation of temperature with OC in the coarse mode suggests coagulation of secondary organic particles with coarse nitrate, and increasing emissions of biogenic particles.
- **SO_4^{-2}:** High correlation of temperature with sulfate may also result from increased transport of diesel emissions from the central LA Basin to Claremont, and increased contributions from both marine and continental sulfate.
- **NO_3^-:** Coarse mode nitrate observed during the warming period may result from reactions of sea salt with photochemically produced HNO_3.

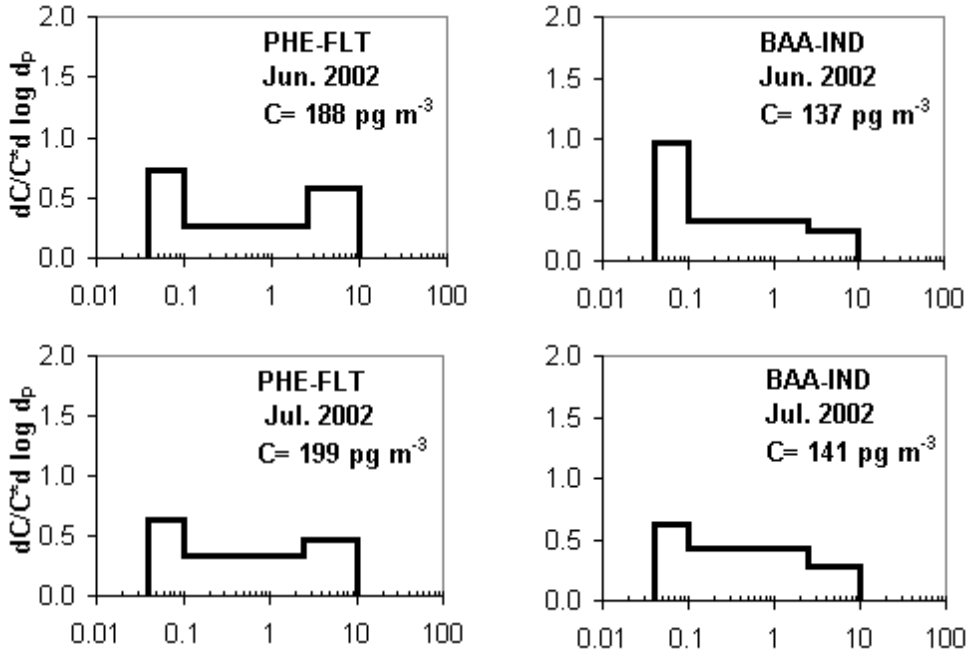

Fig. 1. Size distributions and total mass concentrations (C) of PAH groups PHE-FLT and BAA-IND measured in June and July, 2002 in Claremont, CA. Data obtained from monthly composites.

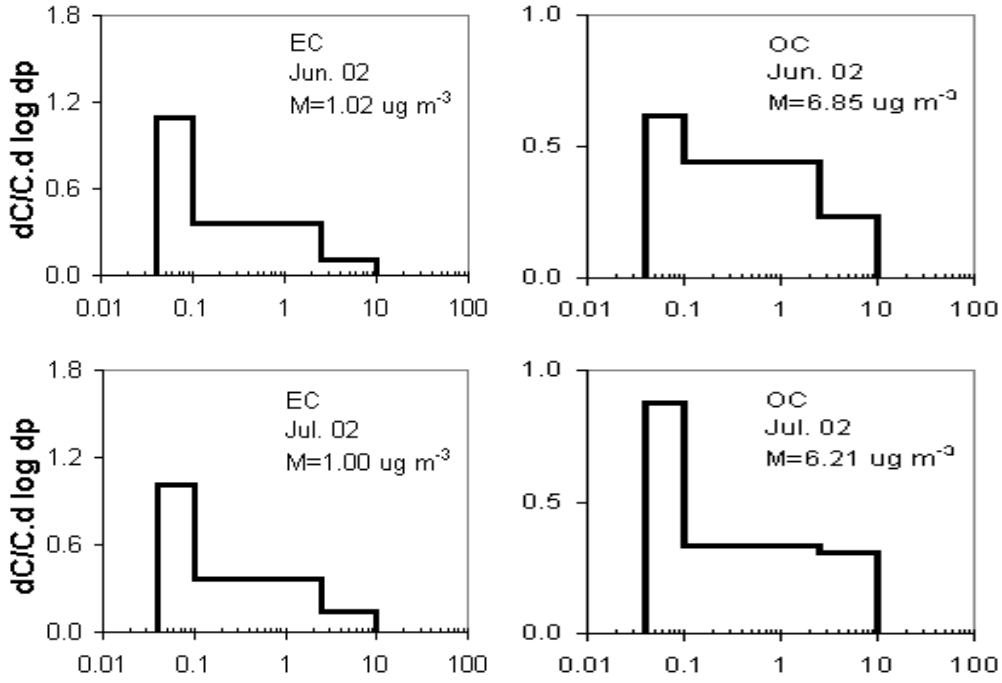

Fig.2. Size distributions and total mass concentrations (M) of EC and OC measured in June and July, 2002 in Claremont, CA. Data obtained from monthly composites.

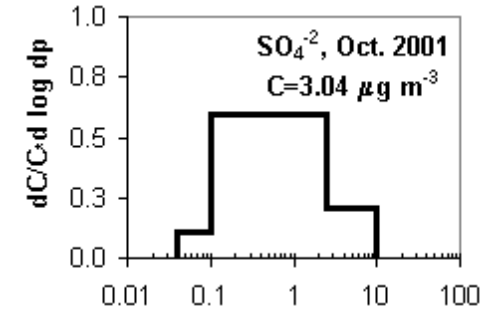
dC/Cd log dp
1.0
0.8
0.5
0.3
0.0
0.01
0.1
1
10
100
SO4-2, Oct. 2001
C=3.04 μg m-3

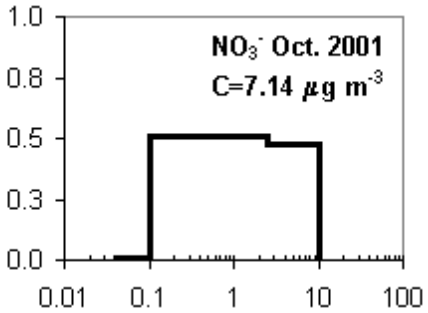
1.0
0.8
0.5
0.3
0.0
0.01
0.1
1
10
100
NO3- Oct. 2001
C=7.14 μg m-3

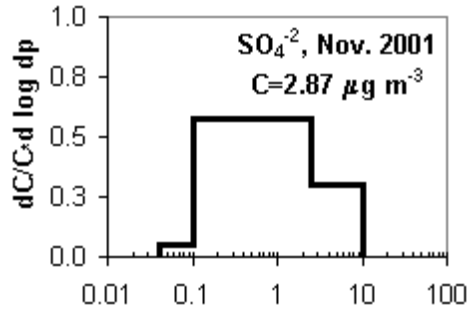
dC/Cd log dp
1.0
0.8
0.5
0.3
0.0
0.01
0.1
1
10
100
SO4-2, Nov. 2001
C=2.87 μg m-3

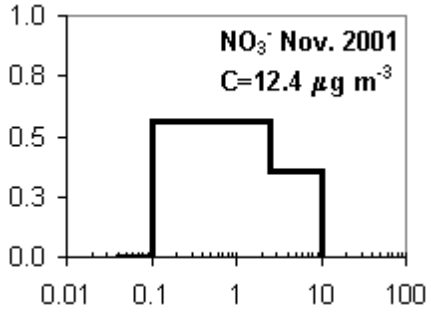
1.0
0.8
0.5
0.3
0.0
0.01
0.1
1
10
100
NO3- Nov. 2001
C=12.4 μg m-3

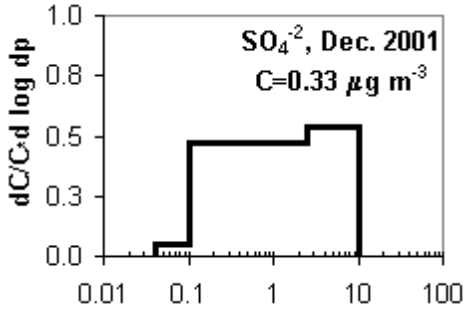
dC/Cd log dp
1.0
0.8
0.5
0.3
0.0
0.01
0.1
1
10
100
SO4-2, Dec. 2001
C=0.33 μg m-3

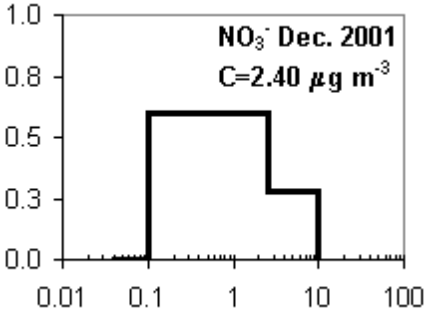
1.0
0.8
0.5
0.3
0.0
0.01
0.1
1
10
100
NO3- Dec. 2001
C=2.40 μg m-3

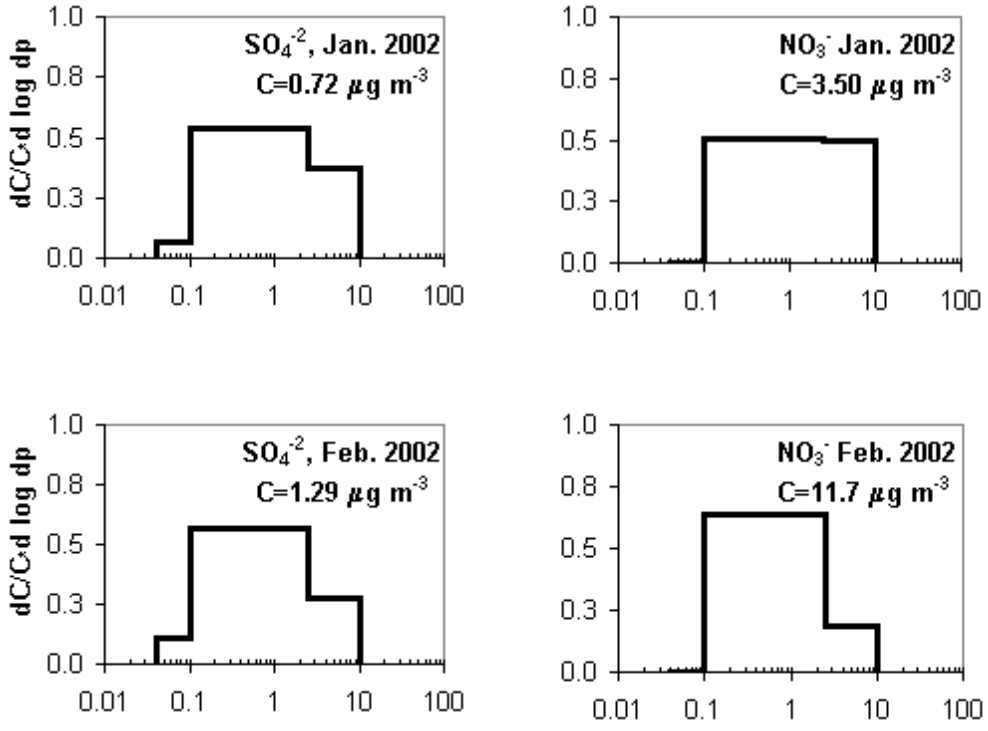

Fig. 3-A. Size distributions and total mass concentrations (C) of SO_4 and NO_3 measured from October 2001, to February, 2002 in Claremont, CA. Data obtained from monthly composites.

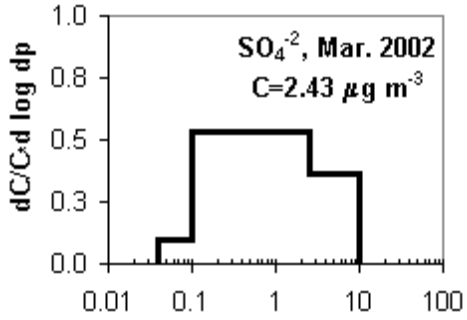
dC/C×d log dp
1.0
0.8
0.5
0.3
0.0
0.01
0.1
1
10
100
SO4-2, Mar. 2002
C=2.43 μg m-3

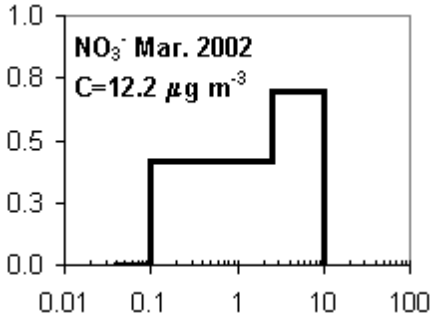
1.0
0.8
0.5
0.3
0.0
0.01
0.1
1
10
100
NO3- Mar. 2002
C=12.2 μg m-3

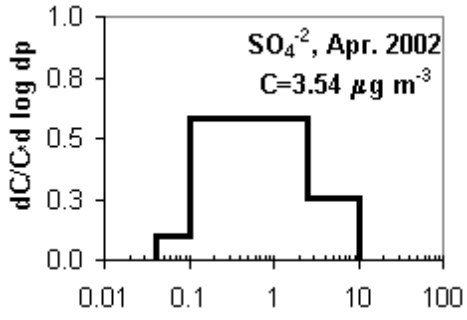
dC/C×d log dp
1.0
0.8
0.5
0.3
0.0
0.01
0.1
1
10
100
SO4-2, Apr. 2002
C=3.54 μg m-3

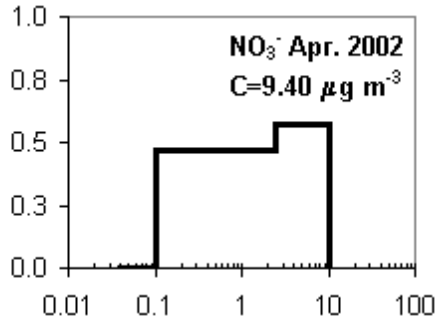
1.0
0.8
0.5
0.3
0.0
0.01
0.1
1
10
100
NO3- Apr. 2002
C=9.40 μg m-3

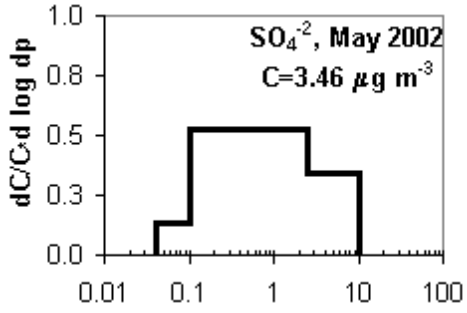
dC/C×d log dp
1.0
0.8
0.5
0.3
0.0
0.01
0.1
1
10
100
SO4-2, May 2002
C=3.46 μg m-3

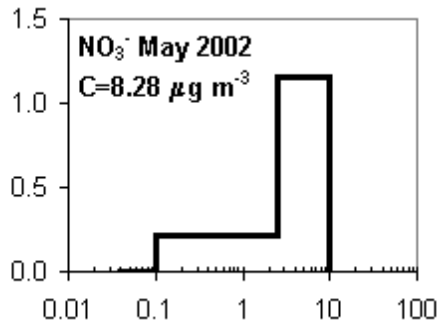
1.5
1.0
0.5
0.0
0.01
0.1
1
10
100
NO3- May 2002
C=8.28 μg m-3

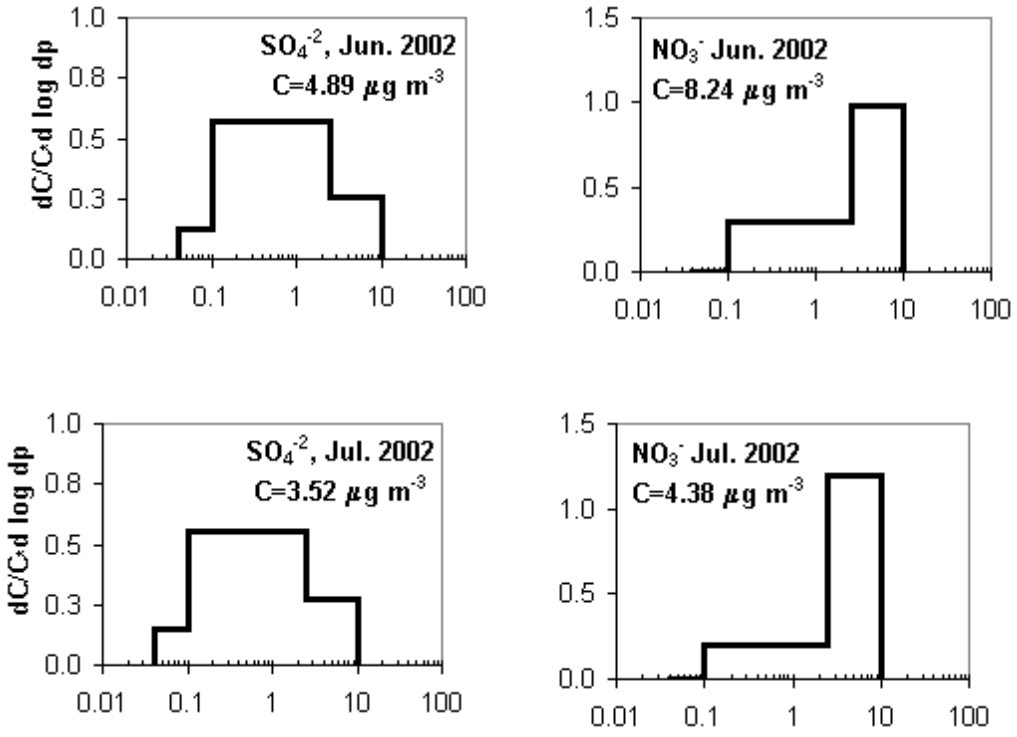

Fig. 3-B. Size distributions and total mass concentrations (C) of SO_4 and NO_3 measured from March to July, 2002 in Claremont, CA. Data obtained from monthly composites.

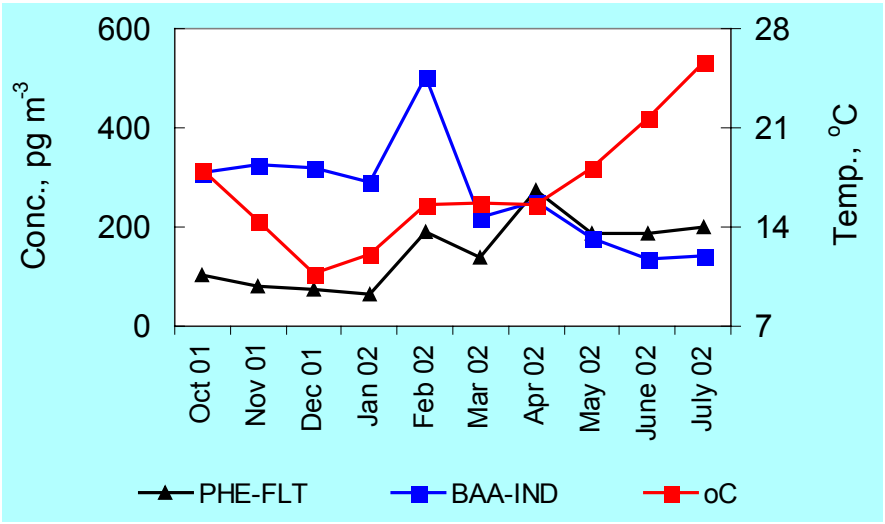

Fig 4. Average monthly temperatures, and seasonal trends of total mass concentrations (M) of PAH groups PHE-FLT and BAA-IND, measured from October, 2001 to July, 2002.

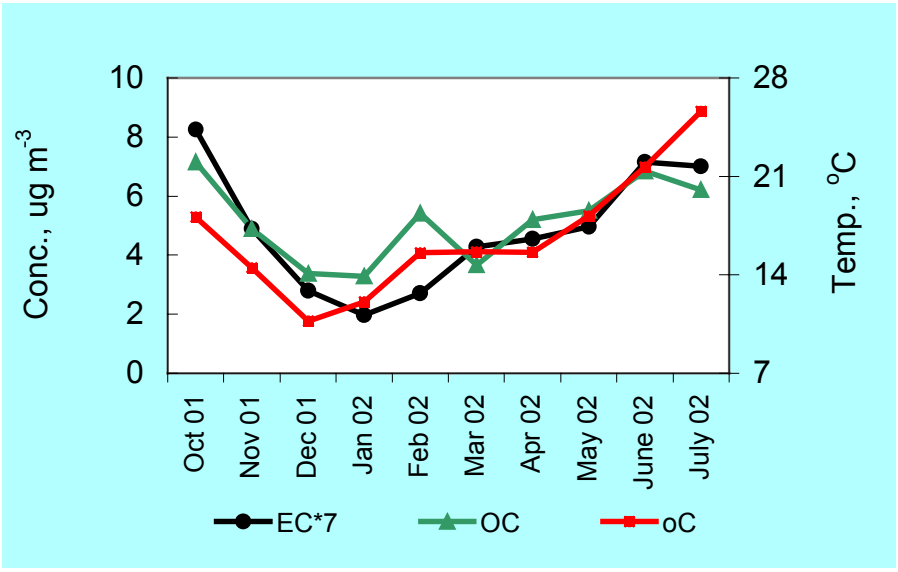

Fig 5. Average monthly temperatures, and seasonal trends of total mass concentrations (M) of EC and OC measured from October, 2001 to July, 2002.

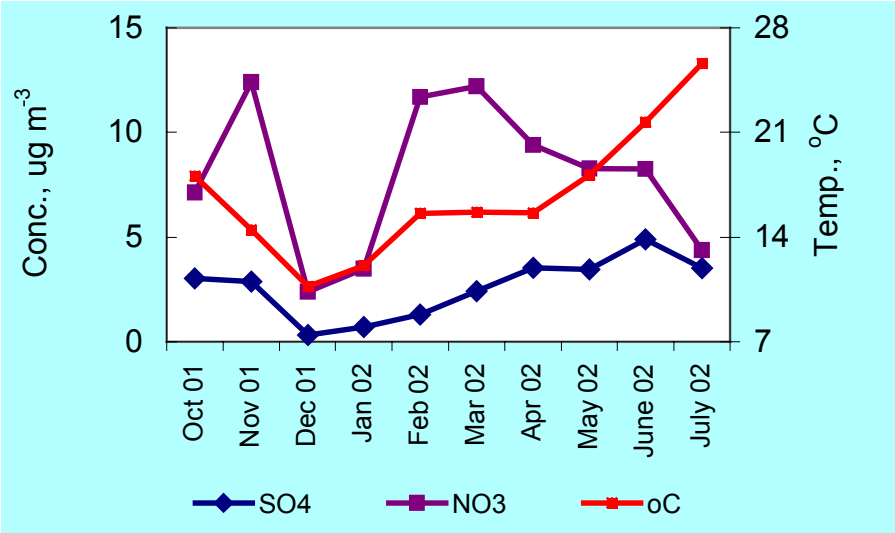

Fig 6. Average monthly temperatures, and seasonal trends of total mass concentrations (M) of SO_4 and NO_3 measured from October, 2001 to July, 2002.

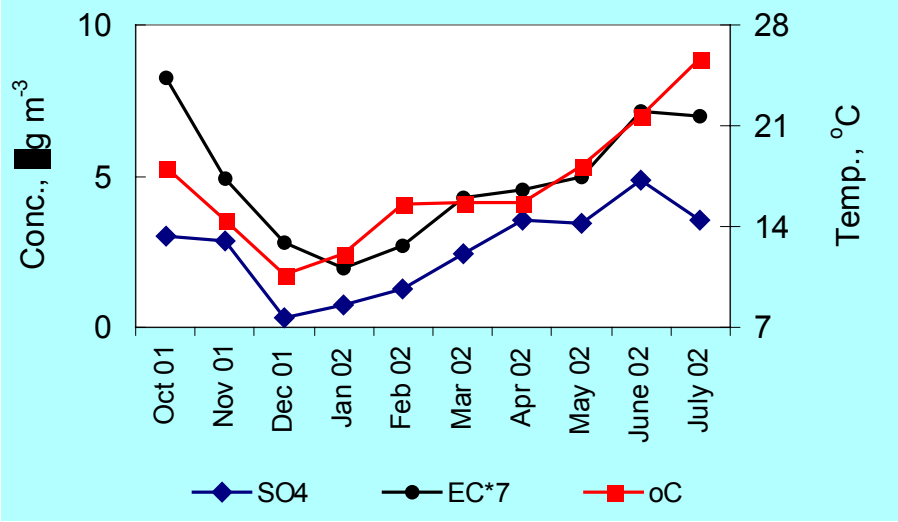

Fig 7. Average monthly temperatures, and seasonal trends of total mass concentrations (M) of SO_4 and EC (*7) measured from October, 2001 to July, 2002

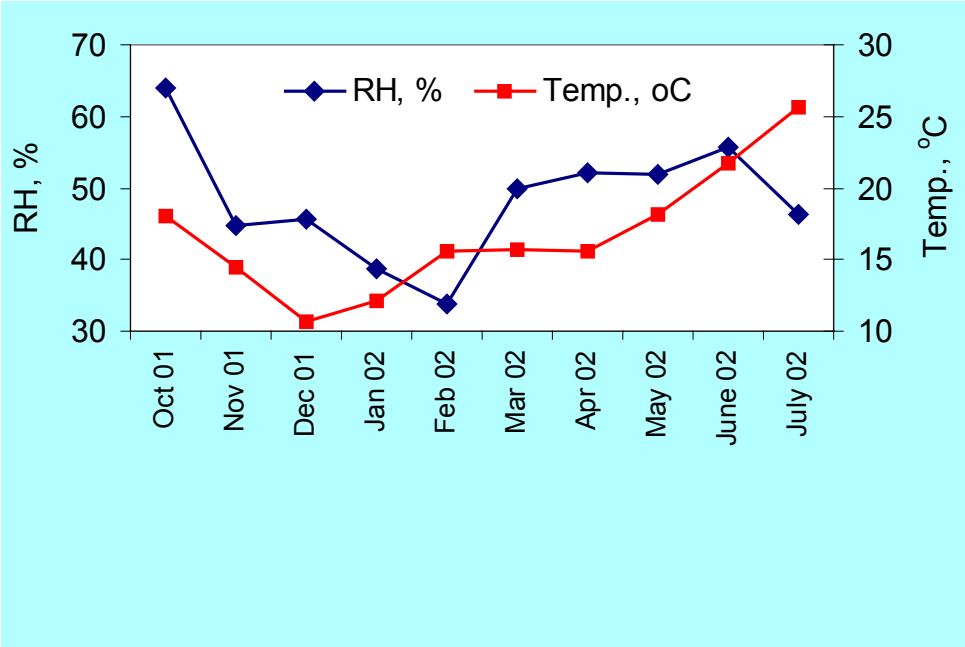

Fig. 8. Average monthly RH and temperature seasonal trends measured from October, 2001 to July, 2002.